ESA CONTRACT REPORT

Contract Report to the European Space Agency

The technical support for global validation of ERS Wind and Wave Products at ECMWF

(July 2007 - June 2008)

November 2008

Authors: Saleh Abdalla and Hans Hersbach

Final report for ESA contract 20901/07/I-EC

European Centre for Medium-Range Weather Forecasts
Europäisches Zentrum für mittelfristige Wettervorhersage
Centre européen pour les prévisions météorologiques à moyen terme

ECMWF

Series: ECMWF - ESA Contract Report

A full list of ECMWF Publications can be found on our web site under:
http://www.ecmwf.int/publications/

Contact: library@ecmwf.int

European Centre for Medium Range Weather Forecasts
Shinfield Park, Reading, RG2 9AX, England

Contract Report to the European Space Agency

The technical support for global validation of ERS Wind and Wave Products at ECMWF (July 2007 - June 2008)

Authors: Saleh Abdalla and Hans Hersbach

Final report for ESA contract 20901/07/I-EC

European Centre for Medium-Range Weather Forecasts

Shinfield Park, Reading, Berkshire, UK

November 2008

	Name	Company
First version prepared by (29 July 2008)	S. Abdalla H. Hersbach	ECMWF ECMWF
Quality Visa	P. Bougeault	ECMWF
Application Authorized by	P. Féménias	ESA/ESRIN

Distribution list:

ESA/ESRIN
Pierre Féménias
Wolfgang Lengert
Pascal Lecomte
Nuno Miranda
ESA ESRIN Documentation Desk

SERCO
Raffaele Crapolicchio
Giovanna De Chiara

ESA/ESTEC
Paul Snoeij
Evert Attema

EUMETSAT
Julia Figa-Saldaña
Hans Bonekamp

ECMWF
HR
Division Section Heads
Ocean Wave Group

Abstract

Contracted by ESA/ESRIN, ECMWF is involved in the global validation and long-term performance monitoring of the wind and wave Fast Delivery products that are retrieved from the Radar Altimeter (RA), the Synthetic Aperture Radar (SAR) and the Active Microwave Instrument (AMI), on-board the ERS spacecraft. Their geophysical content is compared with corresponding parameters from the ECMWF atmospheric and wave model as well as in-situ observations (when possible). Also, tests on internal data consistency are performed.

The project (18212/04/I-OL), which ran from 1 April 2004 to 30 June 2008, is the continuation of previous contracts initiated with ESA/ESRIN and ESTEC. This note presents the final report on the activities performed within the scope of this contract.

An ERS-2 on-board failure in January 2001 degraded attitude control. It had a negative, though acceptable, effect on the quality of the RA and SAR related products; however, a detrimental effect on AMI scatterometer winds. The problems in attitude control were gradually resolved, and since August 2003 the quality of all products is nominal. After 21 June 2003, ERS-2 lost its global coverage permanently due to the failure of both on-board tape recorders. However, the remaining coverage (North Atlantic and western coasts of North America and at a later stage the Southern Ocean, the coasts of East Asia, the northeastern parts of the Indian Ocean and the southern coasts of Africa) provides valuable data for assimilation in atmospheric models. Major part of this report is dedicated to that period.

Furthermore, an overview evaluation of the wind and wave products from the entire ERS mission was carried out (see Abdalla and Hersbach, 2006 and 2007). The products involved are the fast delivery AMI scatterometer wind and SAR wave mode spectra and the off-line ocean product (OPR) wind and wave data from both ERS-1 and ERS-2 missions.

1 Introduction

The ERS mission is a great opportunity for the meteorological and ocean-wave communities. The wind and wave products from ERS-1/2 provide an invaluable data set. They form a benchmark against which model products can be validated. In addition, they are assimilated in the models to improve the predictions. On the other hand, consistent model products, especially first-guess products, can be used to validate and monitor the performance of the satellite products.

The European Centre for Medium-Range Weather Forecasts (ECMWF) has been collaborating with the European Space Agency (ESA) since the beginning of the ERS-1 mission in performing the global validation and long-term performance monitoring of the wind and wave products. These products are retrieved from three instruments, defining three Fast Delivery (FD) products that are received at ECMWF in BUFR format. Significant wave height and surface wind speed (URA product) are obtained from the Radar Altimeter (RA). Ocean image spectra (UWA product) are from the Synthetic Aperture Radar (SAR). Surface wind speed and direction (UWI product), finally, are retrieved from the Active Microwave Instrument (AMI) scatterometer. In-house developed monitoring tools are used for the comparison of these products with corresponding parameters from the ECMWF atmospheric (IFS) and wave (ECWAM) models (IFS Documentation, 2004). Whenever possible, these tools include a comparison with in-situ measurements. In addition, tests are performed on the internal consistency of the underlying observed quantities measured by the three instruments.

This support has been carried out within the framework of several consecutive contracts with ESA. The current contract (18212/04/I-OL), which is supervised by the European Space Research Institute (ESRIN), ran from 1 April 2004 to 30 June 2008. Findings from the monitoring activities described above are summarized in monthly or cyclic (depending on the product) data quality and validation reports. These reports are sent

regularly to ESRIN. Besides giving an overview on instrument performance and scientific interpretation, these reports also include recommendations to ESA for refinements of calibrations, further algorithm development and model tuning. Such recommendations are based on a long-term analysis of the relevant parameters.

In addition to these monitoring activities, dedicated studies on data quality and related scientific research have been carried out. These embrace, among others, collocation studies, algorithm development and the incorporation of ERS wind and wave data in the operational ECMWF assimilation system. As a result, ERS altimeter wave heights have been assimilated in the ECMWF wave model since 15 August 1993 (Janssen *et al.* 1997). It was replaced by ENVISAT Radar Altimeter-2 (RA-2) on 22 October 2003. Scatterometer winds were introduced in the atmospheric variational assimilation system on 30 January 1996 (for a description of its impact, see Isaksen and Janssen 2004). It was re-introduced on 8 March 2004 (Hersbach *et al.* , 2004), after the suspension in January 2001. The assimilation of SAR wave mode spectra in the ECMWF wave model, on the other hand, was realised on 13 January 2003. ERS-2 SAR assimilation was replaced by ENVISAT Advanced Synthetic Aperture Radar (ASAR) Level 1b wave mode spectra on 1 February 2006.

Since the ERS mission is approaching the end of its lifetime, it was thought opportune to make a review of the quality of the various products from both ERS-1 and ERS-2 satellites. Those products are the fast delivery (FD) scatterometer wind (UWI) product, FD SAR Wave Mode (UWA) product and both FD (URA) and the off-line OPR (Ocean Product) altimeter wind and wave products. The results of this exercise can be found in Abdalla and Hersbach (2006 and 2007)

This document presents the final report of the present contract. It provides a focus on the operational performance of the wind and wave products over the last few years. Furthermore, an overview assessment of wind and wave products from the ERS mission since the start of the mission.

In Section 2, the performance of altimeter FD URA data in the North Atlantic will be considered. An overview of the performance of the SAR significant wave height in the North Atlantic will be presented in Section 3, and of UWI wind data in Section 4. In Section 5, conclusions are formulated, and the report ends with a list of ECMWF model changes since November 2000.

Acronyms

AMI	Active Microwave Instrument
ASPS	Advanced Scatterometer Processing System
AOCS	Attitude and Orbit Control System
ASAR	Advanced Synthetic Aperture Radar
ASCAT	Advanced SCATterometer
ASCII	American Standard Code for Information Interchange
BUFR	Binary Universal Form for the Representation of meteorological data
CERSAT	French ERS Processing and Archiving Facility (Centre ERS d'Archivage et de Traitement)
CMEDS	Canadian Marine Environmental Data Service
CMOD	C-band Geophysical MODel function
EBM	Extra Back-up Mode
ECMWF	European Centre for Medium-range Weather Forecasts
ECWAM	ECMWF WAve Model (an enhanced version of WAM model)
ENVISAT	ENVIronmental SATellite
ERS	European Remote sensing Satellite
ESA	European Space Agency
ESACA	ERS Scatterometer Attitude Corrected Algorithm
ESTEC	European Space research and TEchnology Centre
ESRIN	European Space Research INstitute
FD	Fast Delivery product
FEEDBACK	data to which information on usage in the ECMWF assimilation system has been added
FG	ECMWF First Guess with a time resolution of 3 hours
FGAT	First Guess at Appropriate Time
GMF	scatterometer Geophysical Model Function
GTS	Global Telecommunication System
HRES	High RESolution
IDL	Interactive Data Language
IFREMER	French Research Institute for Exploitation of the Sea (Institut français de recherche pour l'exploitation de la mer)
IFS	ECMWF Integrated analysis and Forecast System
JPL	Jet Propulsion Laboratory
KNMI	Koninklijk Nederlands Meteorologisch Instituut
LRDPF	Low Rate Data Processing Facility
LBR	Low Bit Rate
MPI	Max-Planck-Institut for meteorology, Hamburg
NESDIS	National Environmental Satellite Data and Information Service
NDBC	U.S. National Data Buoy Center
NH	Northern Hemisphere
NRES	Nominal RESolution
NRT	Near-Real Time
OPR	(ERS Radar Altimeter) Ocean PRoduct

QC	Quality Control
QSCAT-1	QuikSCAT Scatterometer geophysical model function
RA	Radar Altimeter
RA-2	(ENVISAT) Radar Altimeter-2
RMSE	Root-Mean Square Error
SAR	Synthetic Aperture Radar
SH	Southern Hemisphere
SI	Scatter Index
STDV	STandard DeViation (of the Difference)
SWH	Significant Wave Height
UKMO	UK Met Office
URA	User FD Radar Altimeter product
UTC	Coordinated Universal Time
UWA	User FD SAR WAve product
UWI	User FD scatterometer WInd product
WAM	third-generation ocean-WAve Model
WVC	scatterometer Wind-Vector Cell (node)
WMO	World Meteorological Organization
ZGM	Zero-Gyro Mode

2 The Radar Altimeter URA Product

Each URA (User fast delivery Radar Altimeter) product is sampled at 7 km along the satellite ground track. First the altimeter data stream is divided into sequences of 30 individual neighbouring observations. Erroneous and suspicious individual observations are removed and the remaining data in each sequence are averaged to form a representative super-observation, provided that the sequence has at least 20 ”good” individual observations. Then, further monitoring is performed with respect to these super-observations, which, for this purpose are collocated with ECMWF model parameters and buoy data. Focus is on URA backscatter, URA wind speed and URA significant wave height.

2.1 Data Coverage after June 2003

The loss of the global coverage due to the failure of the on-board low-bit rate tape recorders in June 2003 reduced the number of observations received at ECMWF to about 13% of the full coverage data volume as can be seen in Figure 1 which shows the daily rate of total number of the altimeter super-observations processed at ECMWF. Assessment of the long-term quality of the product after the loss of the global coverage can not be done by comparing it with statistics when there was full coverage. For practical reasons it is not easy to re-process the product over a rather long period for the exact area under current coverage. Instead, readily available long-term statistics for the closest region is considered for comparison. The region covering the extra-tropical Northern Atlantic (north of latitude 20°N) is used as a common area with almost complete coverage before and after the loss of the global coverage. The 7-day running average of daily number of altimeter super-observations in the North Atlantic since the beginning of year 2000 is shown in Figure 2. It is clear that the current coverage in the North Atlantic is slightly lower than the usual coverage. The missing coverage is towards the southern edge of the region as can be seen in Figure 3. Comparing the coverage in Figure 3 with the corresponding one for last year (e.g. Figure 3 of Abdalla and Hersbach, 2007), it is possible to notice the extra coverage around the southern parts of Africa due to the addition of the ground station at Johannesburg since May 2008. The further reduction of coverage between the equator and latitude 20°N in the western parts of the Atlantic and the eastern parts of the Pacific cannot be missed. For the URA product, we will focus our attention on the quality of the altimeter products for the current coverage or specifically in the North Atlantic.

2.2 Monitoring of URA Significant Wave Height in the North Atlantic

As usual, URA significant wave heights (SWH) are rather stable and of good quality, apart from the overestimation of small SWH values. Figure 4 shows the time history of the 7- and 365-day running averages of the daily bias between the altimeter and the ECMWF operational model wave heights in the North Atlantic since the beginning of year 2000. After excluding the apparent anomalous altimeter behaviour during March-April 2000 and February 2001 one can distinguish a seasonal cycle of bias in Figure 4 with a minimum value taking place around April-May and a maximum value occurring around October-November before the loss of the global coverage. This seasonal cycle became stronger after the loss of the global coverage with the minimum and maximum values shifted to cover the whole winter and summer, respectively. Although it is difficult to pinpoint the reason for the stronger cycle, recent model changes like the unresolved bathymetry treatment introduced on 9 March 2004 and the change of wave model dissipation introduced on 5 April 2005 are possible candidates. Another possible reason could be related to the uncovered part towards the southern edge of the area (see Figure 3) which shows less variability than the higher latitudes. The 365-day running average in Figure 4 displays a clear general trend of reduced bias over the years as well. The bias changed sign during the last three years indicating that the model wave heights became higher than the altimeter. These changes are

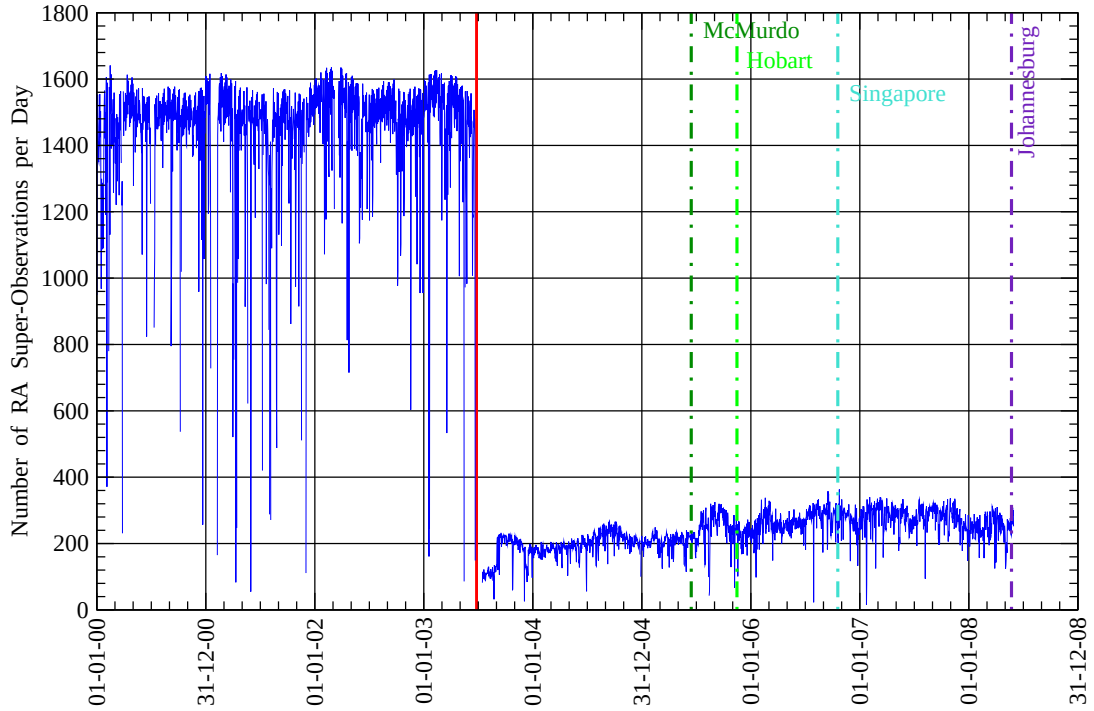

Figure 1: Time history of the total number of ERS-2 altimeter super-observations processed at ECMWF per day since 1 January 2000. Date of loss of global coverage is represented by a red thick vertical line.

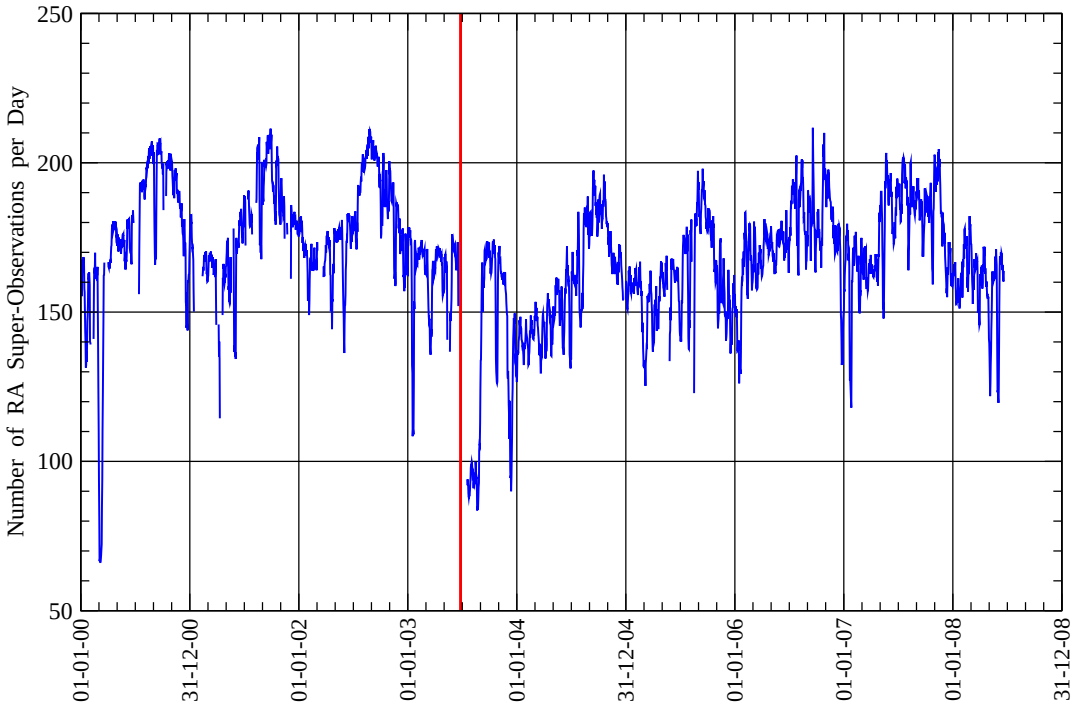

Figure 2: Time history of the 7-day running average of daily number of altimeter super-observations in the North Atlantic since 1 January 2000. Date of loss of global coverage is represented by a red thick vertical line.

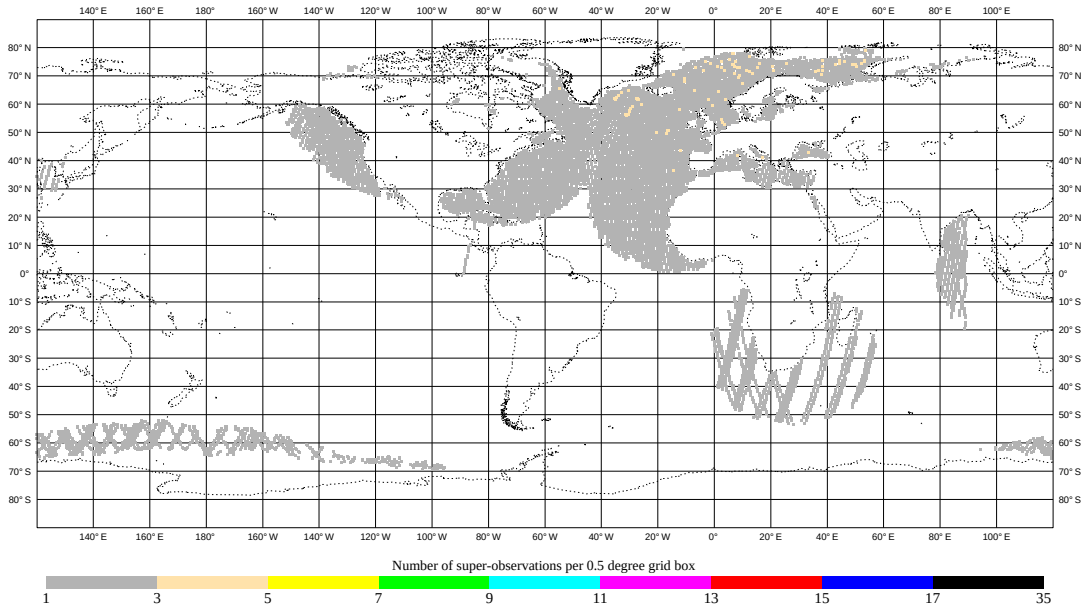

Figure 3: Typical recent ERS-2 radar altimeter monthly coverage (June 2008).

mainly due to the model improvements. Apart from that, the bias between the altimeter and the model wave heights did not suffer any abrupt changes after the loss of the global coverage.

Figure 5 shows the time history of the 7- and 365-day running averages of the daily scatter index (SI) of the altimeter significant wave height with respect to the ECMWF wave model (ECWAM) in the North Atlantic since the beginning of year 2000. Both the seasonal variation (maximum during July-August and minimum during December-January) and the general trend of the reduction in the SI (the 365-day running average) can be seen. Again the seasonal variation seems to be stronger after the loss of global coverage. The higher SI values during July and August 2004 are due to a technical problem that prevented the ENVISAT RA-2 SWH product from being assimilated in the wave model. The continuous reduction of scatter index during the last three years or so is due to the model changes like the revised dissipation formulation in the wave model (April 2005), the high resolution atmospheric model of T799 and the assimilation of Jason altimeter data (February 2006) and the use of model neutral winds to force the wave model.

In summary, it is possible to say that the altimeter significant wave height product is as good as it used to be. Other statistics (not shown) deliver the same message. It is worth mentioning that the ERS-2 altimeter wave height product was assimilated in the ECMWF wave model until it was replaced by the corresponding product from ENVISAT on 21 October 2003.

2.3 Monitoring of URA Surface Wind Speed in the North Atlantic

Before the loss of the global coverage, URA wind speed observations were not as good as the wave heights. They suffered several periods of degraded quality, especially after the start of the problems with the platform gyros in early 2000 (e.g. Abdalla and Hersbach, 2007). The ”sun blinding effect” is responsible for most of

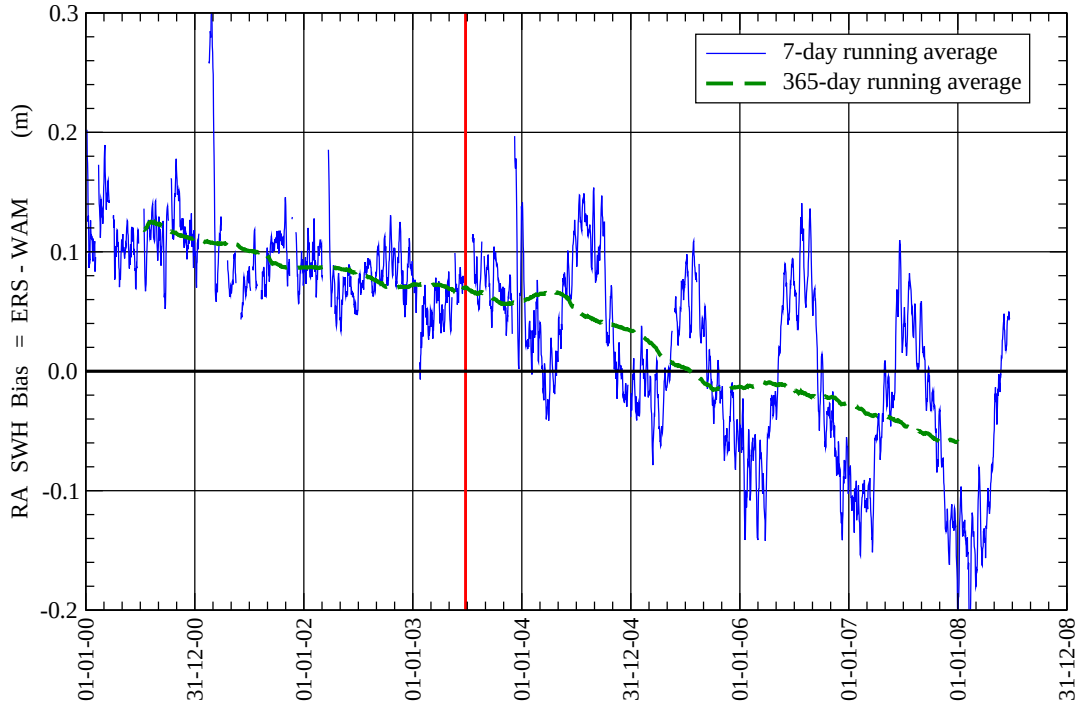

Figure 4: Time history of the 7- and 365-day running average of daily bias of altimeter significant wave height with respect to wave model in the North Atlantic since 1 January 2000. The thick green dashed line shows the bias trend (365-day running average). Date of loss of global coverage is represented by a red thick vertical line.

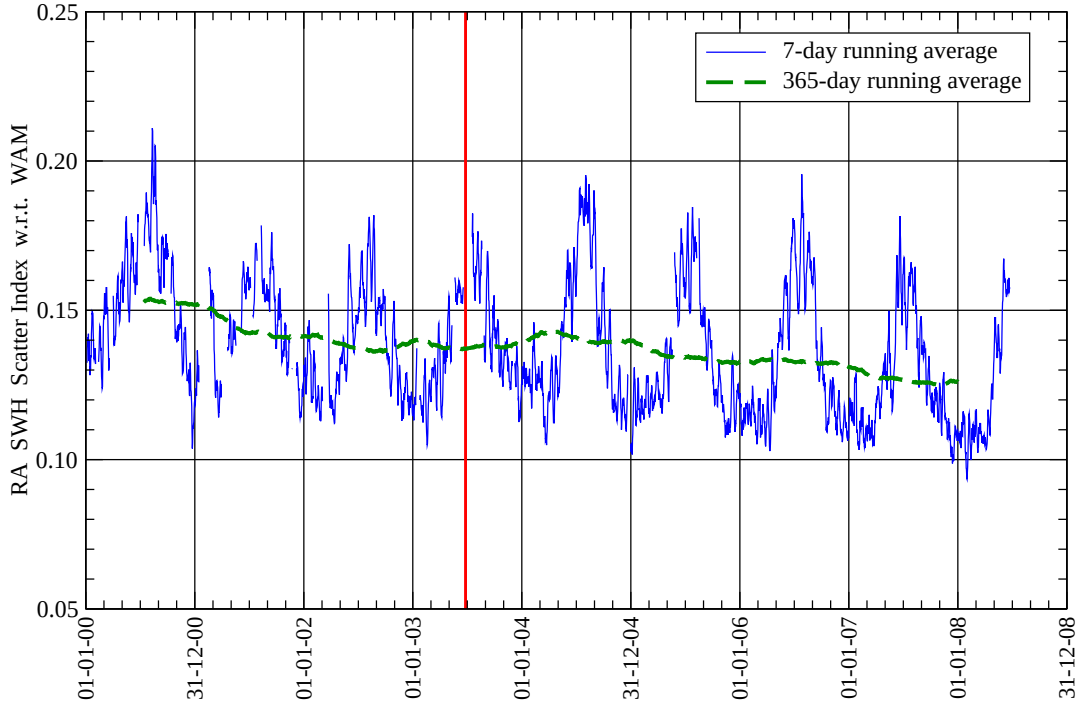

Figure 5: Time history of the 7- and 365-day running average of daily scatter index of altimeter significant wave height with respect to wave model in the North Atlantic since 1 January 2000. The thick green dashed line shows the SI trend (365-day running average). Date of loss of global coverage is represented by a red thick vertical line.

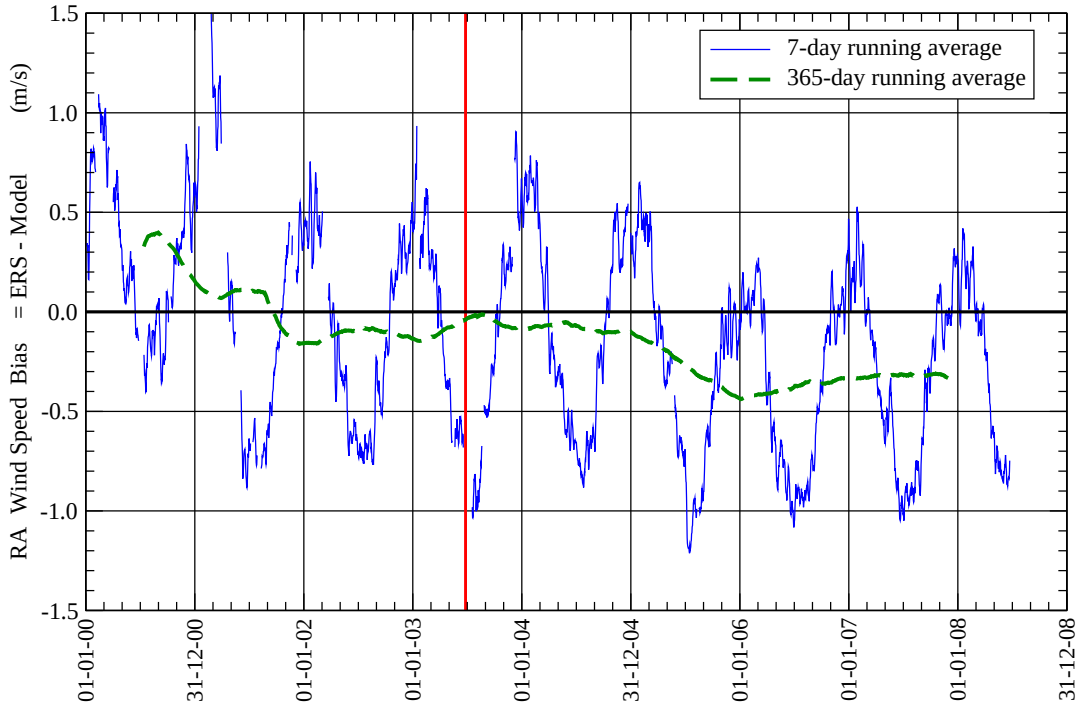

Figure 6: Time history of the 7- and 365-day running average of daily bias of altimeter surface wind speed with respect to the ECMWF atmospheric model in the North Atlantic since 1 January 2000. The thick green dashed line shows the bias trend (365-day running average). Date of loss of global coverage is represented by a red thick vertical line.

the degradation in the Southern Hemisphere (SH) during the period between mid-January to early March each year since year 2000.

Figure 6 shows the time history of the 7- and 365-day running averages of the daily bias of URA surface wind speed with respect to the ECMWF operational atmospheric model in the North Atlantic since 1 January 2000. The wind speed bias in the North Atlantic follows a seasonal cycle with positive bias (maximum) in the Northern Hemispheric (NH) winter and negative (minimum) in the NH summer can be clearly seen. Since early 2001, this seasonal cycle started to be symmetric around the zero line. This can be attributed to the ECMWF high-resolution model T511 implemented on 20 November 2000. The same behaviour continued after the loss of the global coverage. Another drop of bias, is witnessed in the middle of 2005 when the model convection was changed on 28 June 2005. On the other hand, Figure 7 shows the time history of the daily SI of surface wind speed with respect to the ECMWF operational atmospheric model in the North Atlantic since 1 January 2000. The SI follows a weak seasonal cycle with low values occurring during the NH winter and vice versa in summer. The exception to this cycle is the period from early January to early March each year since 2001. This may be due the residual effect of the ”sun blinding effect”. Continuous improvements of the ECMWF operational atmospheric model result in lower wind speed scatter index values between this model and the altimeter. A drop in SI (and bias) in early 2002 can be clearly recognised. This coincides with a model change including the assimilation of QuikSCAT wind speeds. The usual trend of the SI reduction continued after the reduction of ERS-2 coverage. The only exception is the relatively higher scatter index during January and February 2004.

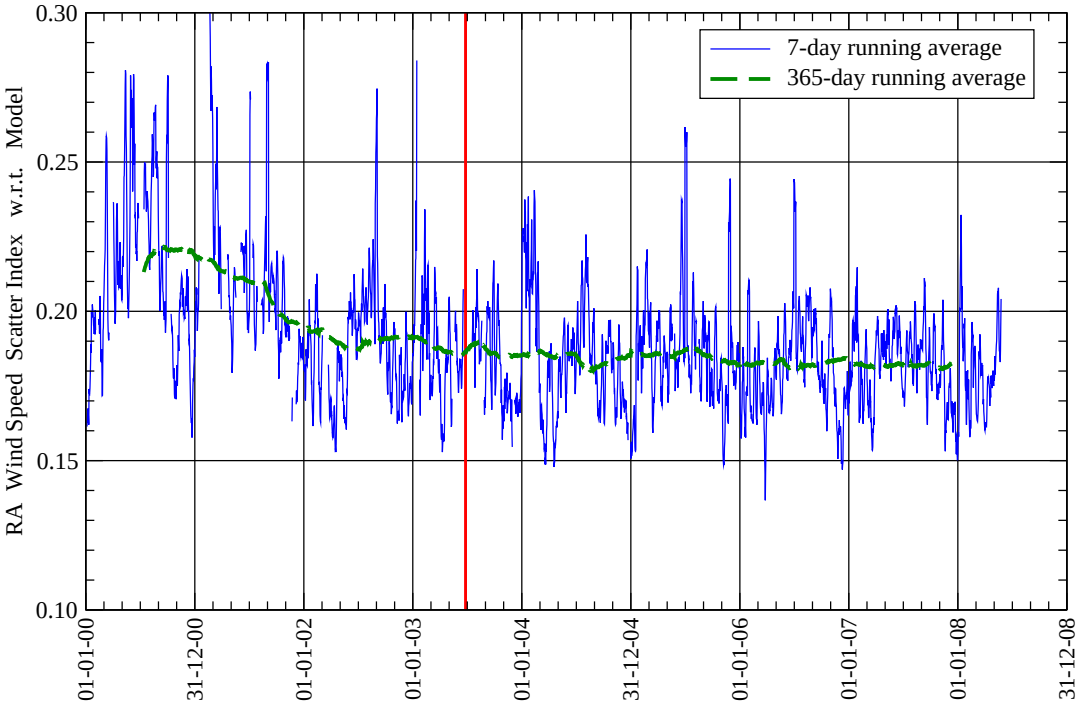

Figure 7: Time history of the 7- and 365-day running average of daily scatter index of altimeter surface wind speed with respect to the ECMWF atmospheric model in the North Atlantic since 1 January 2000. The thick green dashed line shows the SI trend (365-day running average). Date of loss of global coverage is represented by a red thick vertical line.

2.4 Monitoring of URA Altimeter Backscatter

Altimeter backscatter is the raw observation that is translated into surface wind speed. Figure 8 displays the long-term monthly global mean backscatter coefficient values since December 1996. Before the loss of the global coverage, the monthly mean value used to be around 11.0 dB. However, the mean values used to increase to more than 11.4 dB for the month of July in years 1997 to 1999. Those peaks disappeared in year 2000 and later. Instead, the mean backscatter coefficient started to be rather low in the month of February (or March) each year from 2000. This is a direct result from the sun blinding effect.

After the loss of the global coverage, the monthly mean started to have a strong seasonal cycle varies between 10.4 and 12.2 dB. This cycle has a peak during the NH summer (July-August) and a trough during winter (December-January). This is an expected behaviour in the NH. After the extension of the ERS-2 coverage by including more ground stations especially in the SH, the amplitude of the seasonal cycle of mean backscatter coefficient started to get smaller. The impact of including McMurdo, Hobart and Singapore ground stations can not be missed in Figure 8.

3 The Synthetic Aperture Radar (SAR) UWA product

For the UWA product, SAR records are provided at 200 km intervals, each containing an image spectrum for an area of about 5 km x 5 km. Records for which all parameters are within an acceptable range are collocated with ECWAM model spectra. The SAR image spectra are then transformed into corresponding ocean-wave spectra using an iterative inversion scheme based on the forward closed integral transformation (MPI scheme, Hasselmann and Hasselmann, 1991). For this procedure the collocated ECWAM model spectra serve as a first-

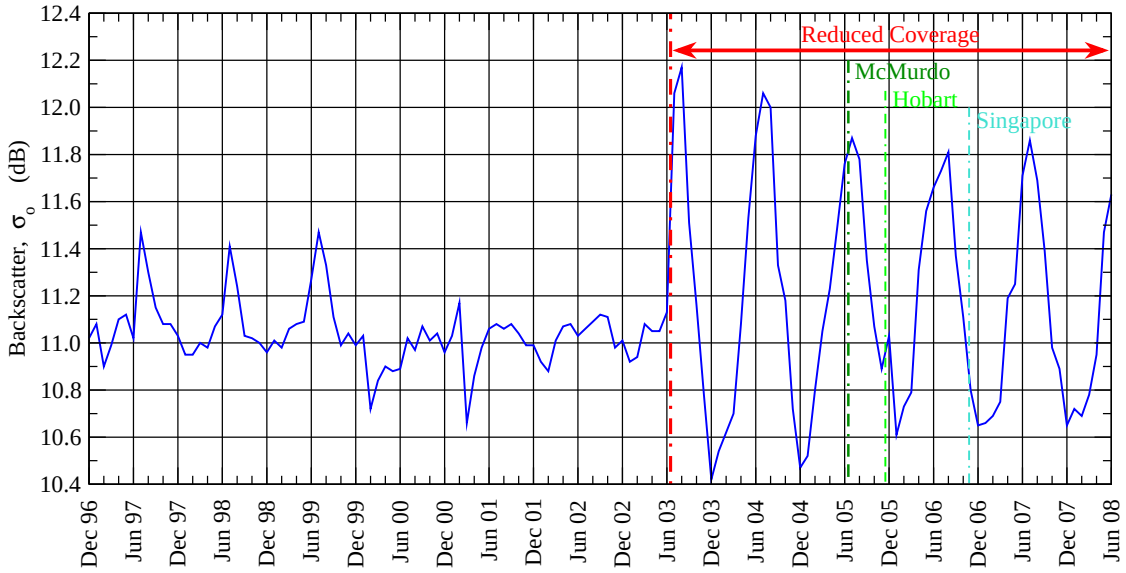

Figure 8: Time history of the monthly global mean of ERS-2 altimeter backscatter coefficient after QC since December 1996.

guess. Depending on the outcome of the inversion process, further QC is applied. Long-term monitoring is based on integrated parameters such as the significant wave height, mean wave period and mean directional spread. Monitoring of the one-dimensional energy spectrum is performed as well.

3.1 ERS-2 SAR Data Coverage after June 2003

The loss of the global coverage due to the failure of the on-board low-bit rate tape recorders in June 2003 reduced the number of observations received at ECMWF to about 13% of the full coverage data volume as can be seen in Figure 9 which shows the global weekly number of SAR wave mode spectra processed at ECMWF. The current ERS-2 SAR coverage can be seen in Figure 10. The extra coverage around the southern parts of Africa (received by Johannesburg ground station) can be clearly seen when comparing Figure 10 with the corresponding one of last year (Figure 20 of Abdalla and Hersbach, 2007). There was an extra reduction of the amount of UWA product processed at ECMWF since the 5th. of February 2008. This reduction is due to higher than usual rejection of the product. Figure 11 shows the time series of the SAR radar incidence angle since the start of 2008. While the incidence angle used to vary within about 0.5° around the nominal value of 23° before the 5th. of February 2008, the range of variability started to be much higher being between 16.3° and 26.5°. Therefore, the high deviations from the nominal value are rejected.

As was done for the altimeter, the extra-tropical Northern Atlantic (north of latitude 20°N) is used for monitoring the FD SAR wave mode UWA product. This is very close to the bulk of the current coverage. The weekly number of SAR wave mode spectra in the North Atlantic since the beginning of the ERS-2 mission is shown in Figure 12. It is clear that the current coverage in the North Atlantic is slightly less than the nominal coverage. The difference is small and is due to the small gap at the southern edge of the North Atlantic. The extra reduction of the amount of valid data since February 2008 is also visible in this region.

The quality of the UWA product in this area (i.e. North Atlantic) is investigated here.

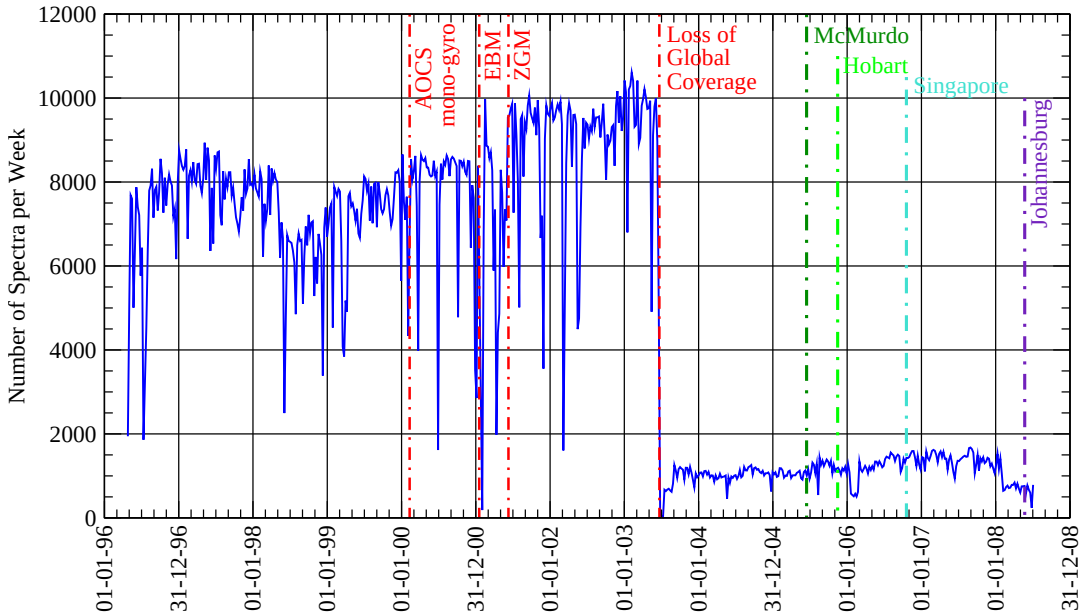

Figure 9: Time history of the global weekly number of ERS-2 UWA spectra during the period since April 1996. Important ERS-2 gyroscope related events are displayed.

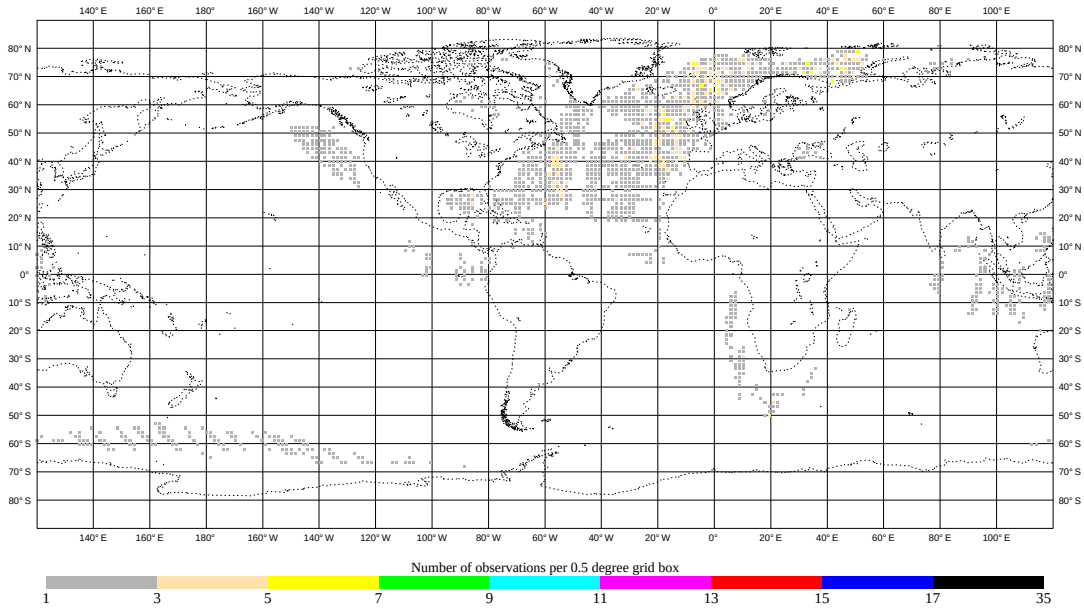

Figure 10: Typical recent ERS-2 SAR wave mode monthly coverage (June 2008).

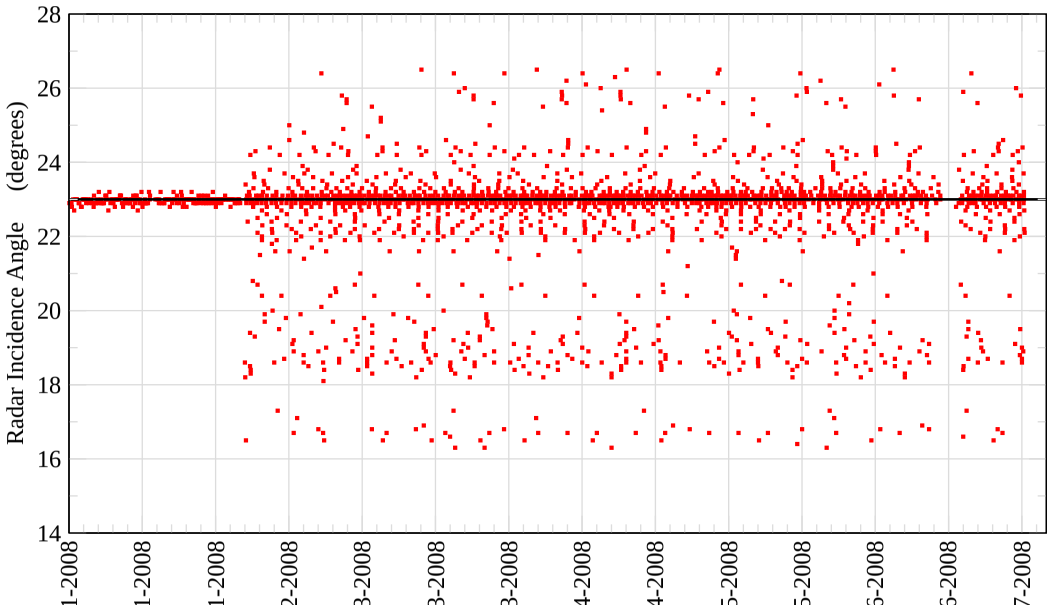

Figure 11: The (thinned) time series of the SAR radar incidence angle since beginning of 2008.

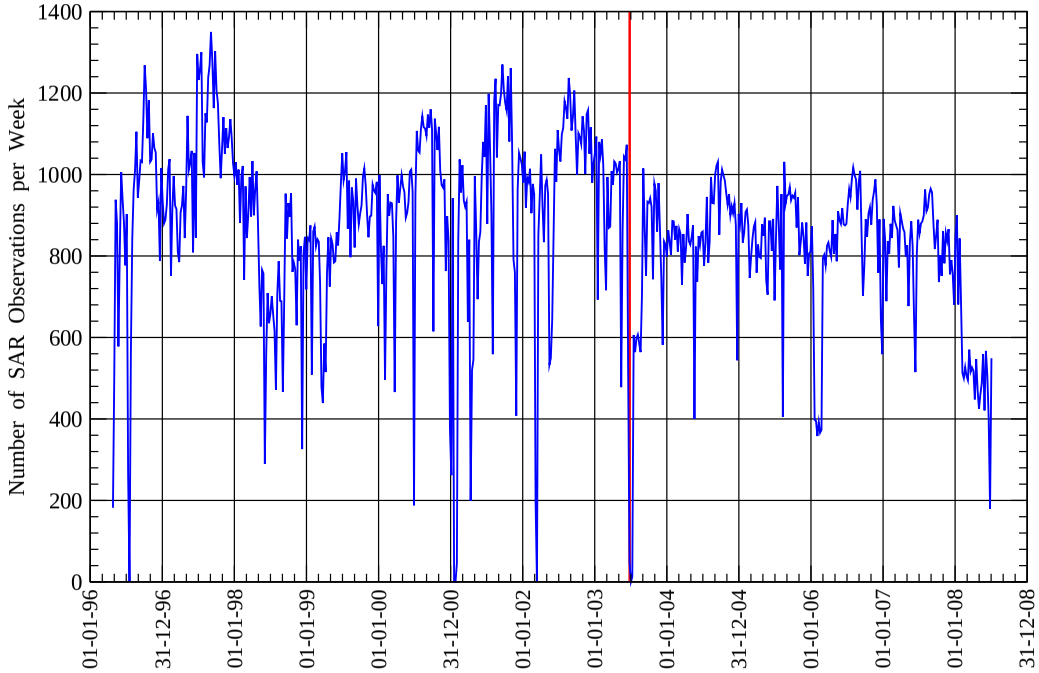

Figure 12: Time history of the weekly number of SAR wave mode spectra in the North Atlantic since 1 January 1996. Date of loss of global coverage is represented by a red thick vertical line.

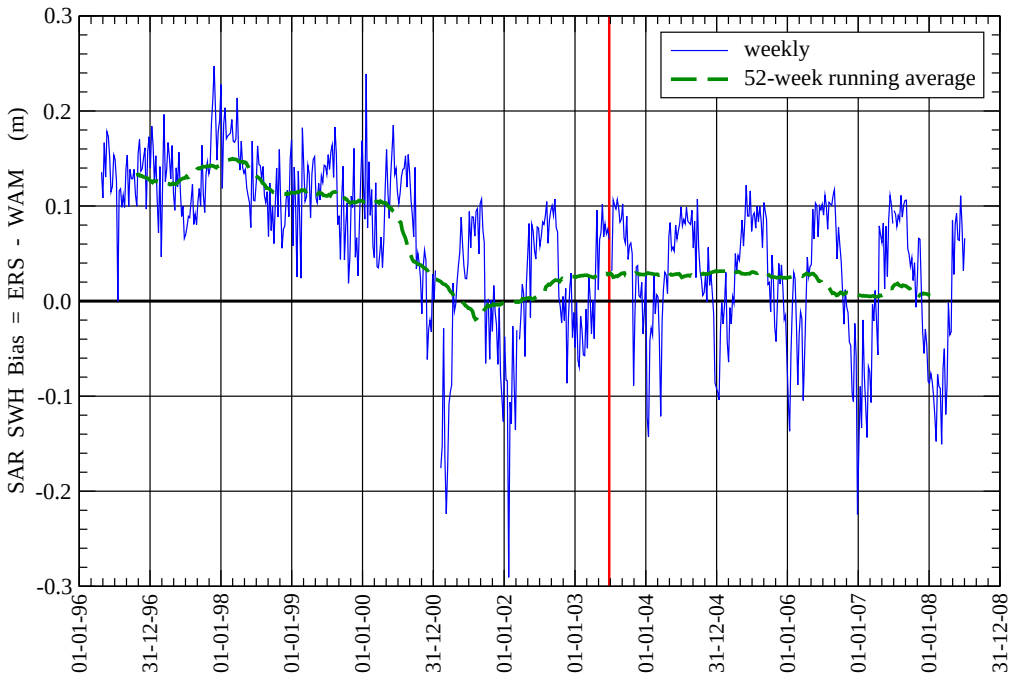

Figure 13: Time history of the weekly bias of SAR wave mode significant wave height with respect to wave model in the North Atlantic since April 1996. 52-week running average is shown by a thick green dashed line. Date of loss of global coverage is represented by a red thick vertical line.

3.2 ERS-2 SAR Wave Height in the North Atlantic

A long-term monitoring of the significant wave height computed from the inverted ERS-2 SAR spectra was performed. It is worthwhile mentioning that on 28 June 1998 the SAR inversion software was unable to properly handle the SAR data with the new calibration procedure introduced around that time. This was fixed with the implementation of the ECWAM model change on 20 November 2000. Furthermore, SAR wave mode data were assimilated in the wave model from 13 January 2003 to 31 January 2006. Other related events are summarised in Abdalla and Hersbach (2007). The most important events are those related to the situation of the gyroscopes. Those events are shown in Figure 9.

Figure 13 shows the time history of the weekly bias of the significant wave height computed from the inverted SAR wave mode spectrum with respect to the model wave height in the North Atlantic since April 1996. By ignoring the period with the inversion bug (from 28 June 1998 to 20 November 2000) and the period with EBM (from 17 January 2001 to mid June 2001), it is possible to recognise a seasonal cyclic variation similar to the altimeter SWH (i.e. with minima during the NH winter and maxima during the summer). It is clear that the bias behaviour since the loss of the global coverage is similar to that of 2-3 years before.

Figure 14 shows the time history of the daily scatter index of the SWH of the inverted SAR wave mode product with respect to the operational wave model in the North Atlantic since April 1996. The period with the inversion bug can be clearly recognised by the high SI values. There tends to be a kind of seasonal cycle (in phase with the bias cycle) of variation in SI after the recovery from the EBM using the ZGM. This seasonal cycle continued after the loss of the global coverage. Furthermore, the general trend of SI reduction continued over the period of limited coverage. Even the errors became smaller than ever; especially during the winter. This may be a consequence of assimilating the SAR wave mode product in the ECMWF operational wave model from 13 January 2003 to 31 January 2006. A step change in SI can not be seen at that specific date. However, the SI peak values started to be the lowest during the NH summer of 2003.

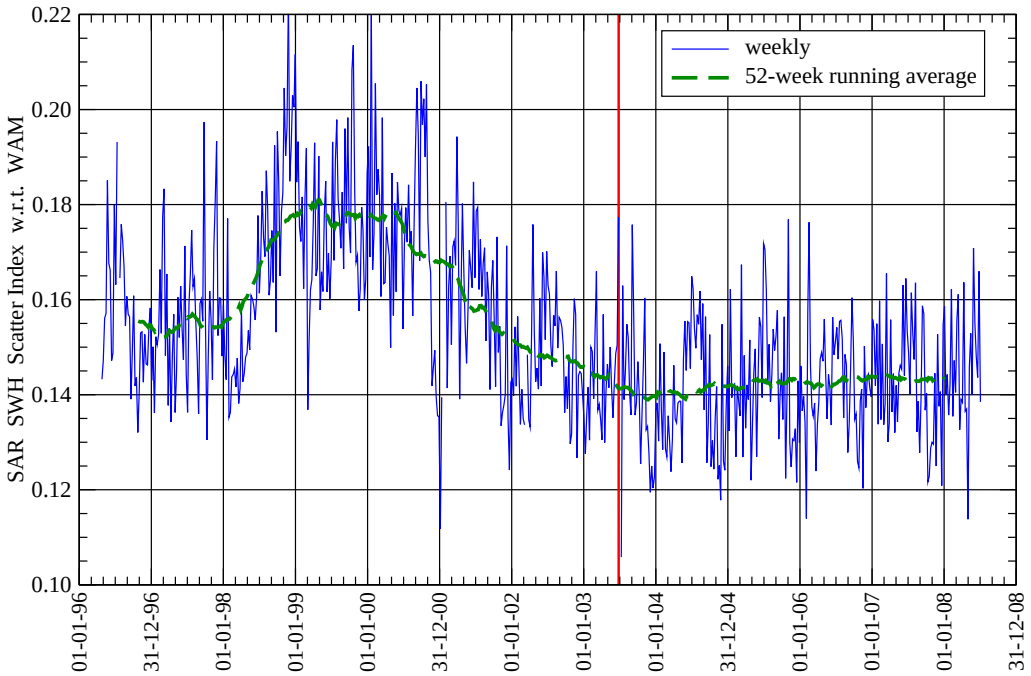

Figure 14: Time history of the weekly scatter index of SAR wave mode significant wave height with respect to wave model in the North Atlantic since April 1996. 52-week running average is shown by a thick green dashed line. Date of loss of global coverage is represented by a red thick vertical line.

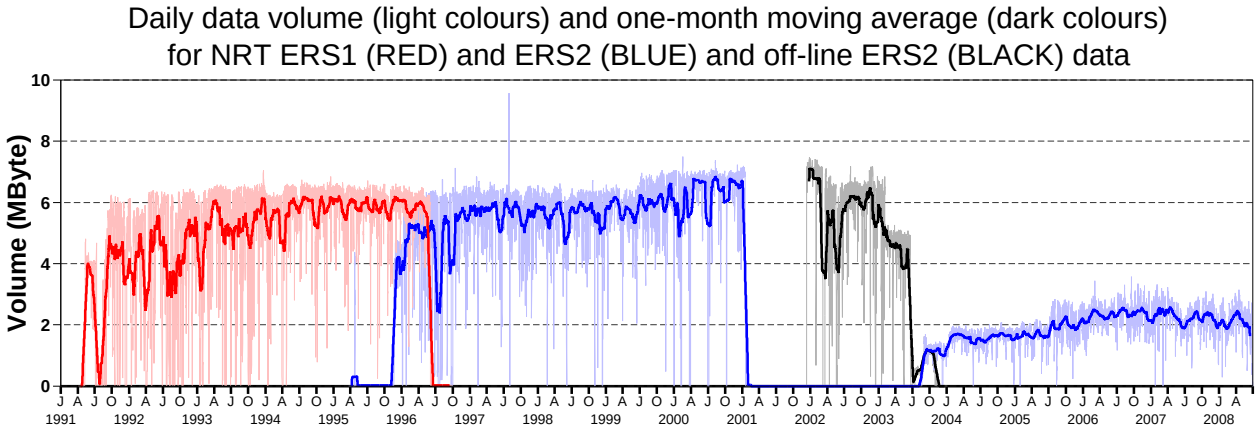

Figure 15: Volume of received ERS-1 and ERS-2 UWI data at ECMWF subject to the data cut-off time in Mbyte per day.

4 The Scatterometer UWI product

4.1 Overview

The AMI instrument on board ERS-2, and previously ERS-1, obtains backscatter measurements from three antennas, illuminating a swath of 500 km, in which 19 nodes, or wind-vector cells (WVC), define a 25 km product (for details on configuration and geometry see Attema, 1986). From these backscatter triplets, two wind solutions are retrieved one of which is reported in a by ESA disseminated near-real time product, called UWI. For this the geophysical model function CMOD4 (Stoffelen and Anderson, 1997) is used.

ERS-1 was launched on 17 July 1991 and has provided scatterometer data from September 1991 until December 1999. At ECMWF, ERS-1 UWI data was received from 9 May 1991 to 3 June 1996 (red curve in Figure 15), i.e., including some pre-launch test data from 9 May to 4 July 1991. In April 1995 ERS-2 was launched and is still operational. At ECMWF some preliminary data was received on 24 April 1995, while operational data flow started on 22 November 1995 (left-hand blue curve in Figure 15). Due to an on-board anomaly in January 2001, ESA was forced to suspend data dissemination between 18 February 2001 and 21 August 2003. However, off-line data was obtained from ESRIN between 12 December 2001 and 7 November 2003 (black curve in Figure 15). Two months before public re-dissemination, ERS-2 had lost its storage capacity of LBR data, including scatterometer data. After this event, data only remained available when in visual contact with a ground station. As a consequence, global coverage was lost for the newly disseminated stream, resulting in much lower data volumes (right-hand blue curve in Figure 15). The subsequent gradual increase in data volume is the result of the stepwise inclusion of new ground stations. For details see Section 4.3.

Within the framework of various contracts with ESA and ESRIN, ECMWF has been monitoring UWI data for a number of years. By passing derived scatterometer winds to the ECMWF operational assimilation system (initially passively, since January 1996 actively), an accurate comparison with model winds can be obtained. Findings of such comparison are, amongst other quality checks, recorded in cyclic reports on 5-weekly intervals. Elements of these reports are described in Section 4.2.

A summary of the monitoring of the entire ERS-2 period will be presented in Section 4.3.

At ECMWF scatterometer data from ERS-1 and ERS-2 have been actively used in the operational integrated assimilation and forecast system (IFS) since January 1996. Before the ERS-2 anomaly in 2001, winds had been determined from CMOD4. However, since this geophysical model function exhibits biases that strongly depend on both incidence angle and wind speed, corrections had been applied (Isaksen and Janssen 2004). After the re-dissemination of the UWI product, scatterometer winds were re-introduced in IFS on 9 March 2004 (Hersbach, *et al.* 2004). Winds were now based on the updated geophysical model function CMOD5, in which most incidence and wind-speed dependent biases were resolved (Hersbach, *et al.* 2007). However, several collocation studies with buoy data (Portabella and Stoffelen, 2007; and Abdalla and Hersbach, 2007) indicated a residual overall bias of around $-0.5\mathrm{m\,s^{-1}}$. This bias was resolved by the development of CMOD5.4 (Hersbach *et al.* , 2007), and winds based on this model function were introduced in IFS on 12 June 2007.

In the near future, plans exist at ECMWF to assimilate scatterometer data as equivalent neutral wind. Such winds allow to take out the effect of stability of the marine atmospheric boundary layer, which clutters the relation between surface stress and 10-metre model wind. Since scatterometer data are thought to be most closely related to surface stress, the introduction of an observation operator for (equivalent) neutral wind is expected to be beneficial. As a first step, a C-band geophysical model function for equivalent neutral winds has been developed (Hersbach, 2008). Some details on this model function, called CMOD5.N will be discussed in Section 4.4.

On 12 June 2007, data from the ASCAT scatterometer on-board MetOp-A was introduced in the operational assimilation suite at ECMWF. Winds are based on CMOD5.4, and due to a difference in calibration between ERS-2 and ASCAT, bias corrections in backscatter and wind speed before respectively after wind inversion are applied (Hersbach and Janssen, 2007). A collocation study between ERS-2 and ASCAT will be presented in Section 4.5.

4.2 5-weekly cyclic UWI ERS-2 monitoring reports

The routine monitoring of the ERS-2 UWI product at ECMWF is summarized in the form of 5-weekly cyclic reports. At ftp://earth.esa.int/pub/SCATTEROMETER/ecmwf_rep, these reports are available from Cycle 41 (start date 14 July 1998) up to, at the time of this writing, Cycle 140 (end date 13 October 2008).

Up to Cycle 60 (nominal period) the UWI product has been compared with ECMWF first-guess winds as available within the assimilation system. These FGAT (first-guess at appropriate time) winds are well collocated with the scatterometer observation time and location. From Cycle 69 onwards, e.g., with the start of the reception of offline data from ESRIN, collocation was performed with archived first-guess wind fields instead (available at 3-hourly resolution; and will be called FG winds). Collocation errors are slightly larger, but on the other hand it enables the monitoring of data that does not pass pre-screening quality control in the operational ECMWF assimilation system.

From Cycle 69 onwards, the quality of winds inverted on the basis of CMOD5 are monitored as well. At ECMWF, such retrieved ERS-2 scatterometer winds have been assimilated from 9 March 2004 until 5 June 2007, when CMOD5 was replaced by CMOD5.4 (see e.g. Section 4.4 of Abdallah and Hersbach, 2007).

The ECMWF scatterometer cyclic monitoring reports contain the following elements:

- An introduction, giving a general summary of the quality of the UWI data and trends w.r.t. previous cycles. Data coverage, and interruptions in data reception are listed. Also, since Cycle 69 (12 November 2001) it is mentioned whether there was an enhancement of solar activity, and whether it could have affected the UWI wind product. Finally, it is informed whether the ECMWF assimilation system has changed and whether this had an anticipated impact on the quality of the ECMWF surface winds.

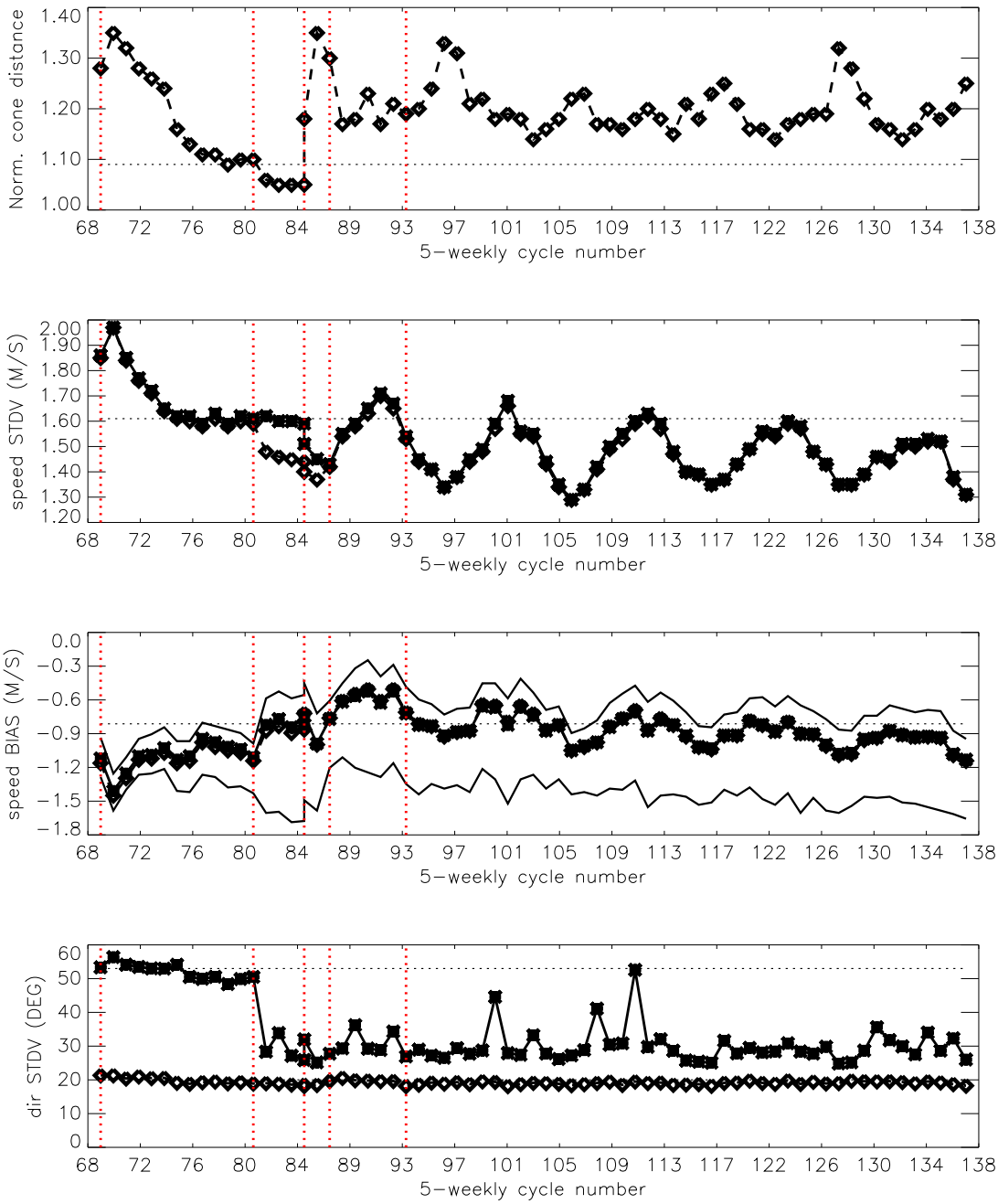

Figure 16: Evolution of the performance of the ERS-2 scatterometer averaged over 5-weekly cycles from 12 December 2001 (Cycle 69) to 30 June 2008 (end Cycle 137) for the UWI product (solid, star) and de-aliased winds based on CMOD4 (dashed, diamond). Results are based on data that passed the UWI QC flags. For Cycle 85 two values are plotted; the first value for the global set, the second one for the regional set (see text for more details). Dotted lines represent values for Cycle 59 (5 December 2000 to 17 January 2001), i.e. the last stable cycle of the nominal period. From top to bottom panel are shown the normalized distance to the cone (CMOD4 only) the standard deviation of the wind speed compared to FG winds, the corresponding bias (for UWI winds the extreme inter-node averages are shown as well), and the standard deviation of wind direction compared to FG.

- A section giving a detailed description of performance during the cycle. It includes the following plots.
- Evolution of 5-weekly averaged performance of the cone distance, bias and standard deviation of UWI and CMOD4 wind speed and direction compared to ECMWF FG winds starting from Cycle 69. The plot for Cycle 137 is given in Figure 16.
- Data coverage and geographical averages of UWI wind speed, and relative bias and standard deviation compared to ECMWF FG winds (Cycle 91 onwards; for Cycle 137, see Figure 17).
- Backscatter (σ_0) bias for the three antennas (fore, mid, aft) as function of WVC (1 to 19) and stratified with respect to ascending and descending tracks:

$$dz = < z > / < z_{\mathrm{CMOD}}(\theta, \mathrm{FGAT}) >, \tag{1}$$

  where $z = \sigma_0^{0.625}$, and θ the WVC and antenna-dependent incidence angle. Note that the in this way estimated bias depends on the underlying model function. Results are produced on the basis of CMOD4. Trends in the inter-node and inter-antenna relationship indicate changes in the antenna patterns, because trends in the normalizing ECMWF winds would appear as integral shifts. Examples are provided in Figures 18 and 20.
- Time series of the difference between the fore and aft incidence angle of node 10 (Cycle 81 onwards), and the UWI k_p-yaw quality flag (Cycle 88 onwards). Asymmetries indicate errors in yaw attitude control.
- Plots of time series of quantities averaged over 6-hourly data batches and stratified w.r.t. six classes of nodes (1-2, 3-4, 5-7, 8-10, 11-14 and 15-19) of
  - The normalized distance to the cone, the fraction of rejected data on the basis of CMOD4 inversion, ESA flags or ECMWF land and sea-ice mask, and the total number of received data over sea.
  - Bias and standard deviation of UWI versus ECMWF first-guess winds for wind speed and direction.
  - The same for CMOD4 winds as inverted at ECMWF from level 1b.
- Global plots of locations where UWI winds were more than 8 $\mathrm{m\,s^{-1}}$ weaker or stronger than ECMWF FG winds (included from Cycle 79). Usually two specific cases are highlighted in a separate plot.
- Accumulated histograms (scatterplots) between UWI and ECMWF first-guess wind speed and direction. Scatterplots for FG winds versus de-aliased CMOD4 winds and CMOD5-based winds have been produced from Cycle 74 onwards. Examples for a one-year accumulation period (July 2007 to June 2008) are presented in Figure 21.
- Time series for at ECMWF assimilated ERS winds (based on CMOD5 or CMOD5.4, rather than CMOD4), and QuikSCAT winds relative to ECMWF FGAT winds for a region covering the North Atlantic and part of Europe (Cycle 94 onwards; for Cycle 137 see Figure 19).

4.3 General Overview for ERS-2

22 November 1995 - 19 March 1996
Pre calibration phase. Large but constant σ_0 biases were encountered.

19 March 1996 - 6 August 1996
End of commissioning phase. A thorough calibration has resulted in revised look-up tables. Scatterometer data

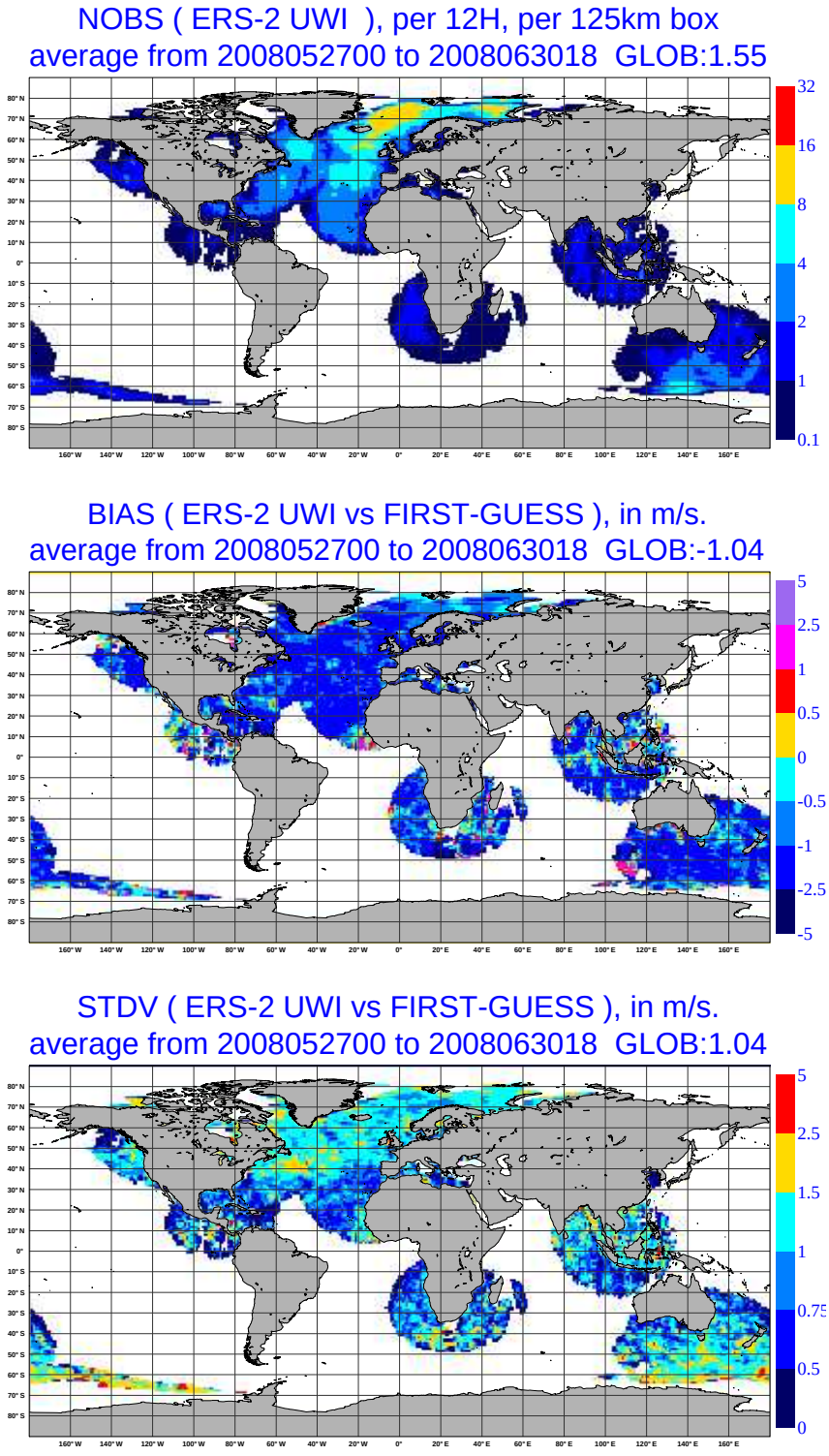

Figure 17: Average number (top) of observations per 12H and per N80 reduced Gaussian grid box (∼ 125 km), relative bias (middle) respectively standard deviation (lower panel) compared to ECMWF FG 10-meter winds, (∼ 125 km) of UWI winds that passed quality control at ECMWF for data in Cycle 137 (27 May to 30 June 2008). Results are only plotted for grid cells that contained at least 5 observations.

from ERS-2 (bias-corrected CMOD4 winds) is included in the ECMWF assimilation system on 1 June 1996, replacing the assimilation from ERS-1 that had been used from 30 January 1996. Details may be found in Isaksen and Janssen (2004).

6 August 1996 - 18 June 1997
On 6 August 1996, the calibration sub-system was switched from nominal side-A to side-B after an on-board anomaly. Since the calibration of side-B was slightly different from side-A, average backscatter level dropped by around 0.2 dB. This issue was resolved on 18 June 1997 with the introduction of an updated calibration in the ground segment processor.

18 June 1997 - 17 January 2001 (Cycle 22 to Cycle 60)
Nominal period. Backscatter values return to old, well-calibrated levels.

The performance of the UWI product is stable, although in the fall of 2000 there are some problems with the functioning of several of the six gyroscopes on-board the spacecraft. On average, backscatter levels are around 0.5 dB too low, leading to winds that are on average 0.7-0.8 $\mathrm{m\,s^{-1}}$ slower than FGAT winds. Although the inter-node and inter-antenna sigma biases are small, the UWI wind-speed bias does depend on node number (from -1.1 $\mathrm{m\,s^{-1}}$ for low to -0.6 $\mathrm{m\,s^{-1}}$ for high incidence angle). It is induced by imperfections in the CMOD4 model function. Standard deviation between UWI and FGAT winds are around 1.6 $\mathrm{m\,s^{-1}}$. For Cycle 59, values of the average cone distance, (UWI - FGAT) and (CMOD4 - FGAT) statistics are displayed by the horizontal dotted lines in Figure 16.

17 January 2001 - July 2001 (Cycle 60 to 65)
As a result of the on-board failure there are no gyroscopes left for the platform's attitude control. The control system is switched to Extra Back-up Mode. The dissemination of scatterometer data is suspended after 2 February 2001; empty cyclic reports are made for Cycles 62 to 68.

July 2001 - 12 December 2001 (Cycle 65 to 69)
Introduction of the Zero-Gyro Mode (ZGM). Satellite pointing is achieved through payload data and the digital earth sensor. Although pitch and roll can be controlled accurately, large errors in the yaw attitude (several degrees) still occur. Such errors especially affect the quality of the scatterometer measurements. Dissemination of scatterometer data remains suspended.

12 December 2001 - 4 February 2003 (Cycle 69 to 81).
Restart of dissemination of UWI data, however, to a restricted group of users only. At ECMWF, the monitoring is resumed. Existing tools are updated where necessary.

Large errors in yaw, which especially seem to occur around periods of enhanced solar activity, have a large negative impact on the data quality. During these events, part of the backscatter signal is destroyed, which, after inversion, results in far too low winds. Peaks of more than -3 $\mathrm{m\,s^{-1}}$ frequently occur, especially in January 2002 (Cycle 70), which marks a period of considerable solar activity. These incorrect data are also visible in the scatter diagrams of UWI versus FG wind speed as anomalously large numbers of collocations between strong ECMWF winds and weak UWI winds. For later cycles the situation improves.

Initially, also extremely large negative biases are observed in the backscatter levels, including data that was less affected by yaw errors. Large inter-node and inter-antenna differences induce large cone distances. The situation is worst for Cycle 70 but later slowly improves. However, the increasing negative bias towards higher nodes remains. In line with the average reduction in σ_0 bias, the cone distance and wind-speed biases gradually improve (see Figure 16).

For the random error of the UWI and CMOD4 wind speeds a similar trend is observed: worst for Cycle 70 (almost 2 $\mathrm{m\,s^{-1}}$) and then first improving rapidly and later stabilizing. From Cycle 75 onwards its level is

around the value obtained for the nominal period (see Figure 16). In general best results are obtained for winds inverted on the basis of CMOD5. Both the negative bias level and standard deviation are smaller for such derived winds.

The performance in wind direction is found to be much less affected. Although initially wind direction performs somewhat worse, at Cycle 72 it is on the level of the nominal period, and after Cycle 75 it has even become better (see lower panel of Figure 16).

4 February 2003 - 22 June 2003 (Cycle 81 to 85)
Start of the validation phase of ESACA, the new processor. Aim of this complete revision of the original LRDPF, was to bring the quality of the UWI product back to its nominal level. It is capable of the interpretation of on-board filter characteristics appropriately according to an estimation of the yaw attitude error. During the test phase, ESACA data is distributed for Kiruna station only, which leads to daily data gaps between approximately 21 UTC and 06 UTC.

The new de-aliasing algorithm, being part of ESACA, (and developed at DNMI) appears to perform well. The UWI winds agree considerably more often with the wind solution that is closest to the ECMWF FG wind direction. Values of standard deviations drop from 50 to less than 30 degrees (see Figure 16).

The UWI winds do not coincide anymore with one of the two solutions from the CMOD4 inversion at ECMWF. At ECMWF inverted CMOD4 winds appear to be of much higher quality than the by ESRIN disseminated UWI winds (see Figure 16). At ESRIN, the cause for this non-ideal situation is tracked down quickly. At the beginning of April 2003 appropriate corrections to ESACA are implemented and since then UWI winds are in line with CMOD4 again (though not yet for Kiruna station; i.e., the discrepancy in winds remains for the data as received at ECMWF). The standard deviation w.r.t. FGAT winds are below 1.50 $\mathrm{m\,s^{-1}}$, i.e., about 0.1 $\mathrm{m\,s^{-1}}$ better than it used to be during the nominal period.

Large fractions of high k_p values are found, especially for nodes at high incidence angles (more than 50%). Consideration between the (UK) MetOffice and ESRIN reveals that there is a problem with the BUFR encoding algorithm. A solution is formulated and implemented (again, not yet at Kiruna).

In the near range the fore and aft antenna show large negative biases in the average backscatter levels. As a result, very large negative wind-speed biases are found for low nodes (-1.6 $\mathrm{m\,s^{-1}}$). At ESRIN its cause is identified and resolved (though, not visible at Kiruna). Apart from the initially large near-range biases, the inter-node and inter-antenna differences in backscatter levels are small. Their level is comparable to that during the nominal period.

The incidence angles between the fore and aft antenna are not equal anymore. They now show a rapid variation in time and peaks up to 7 degrees are observed. This asymmetry is a direct result of errors in yaw attitude. A large anomaly on April 1 2003 (while the Earth was inside a gusty solar wind stream, source: www.spaceweather.com) results in low-quality winds. This event illustrates the potential usefulness of a yaw flag in the UWI product.

Along with improved quality of the CMOD4 winds, the normalized distance to the cone is now below the level of the nominal period.

22 June 2003 - 21 August 2003 (Cycle 85 to 87)
On 22 June 2003 the second Low Bit-Rate recorder on-board ERS-2 fails, and is found to be beyond repair. As the first recorder had become unusable in December 2002, this means that now there is no facility left to store LBR data, which includes scatterometer data. After a data-void period of three weeks, data flow is resumed on 16 July 2003, however, only for observations for which there is a direct contact with a ground station. For the Kiruna test data received at ECMWF, this means that coverage is limited to the Atlantic north of 40°N, making

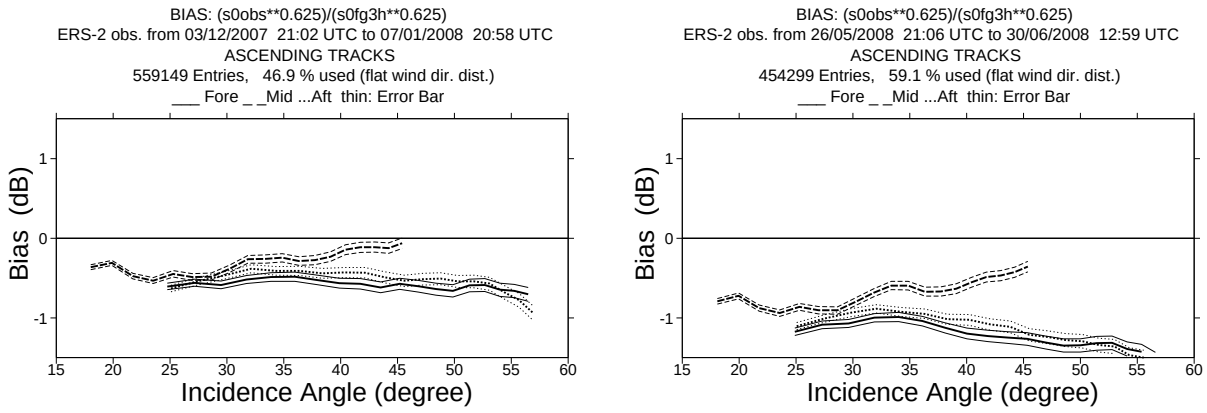

Figure 18: Ratio of $< \sigma_0^{0.625} > / < \mathrm{CMOD4}(\mathrm{FGAT})^{0.625} >$ *converted in dB for the fore antenna (solid line), mid antenna (dashed line) and aft antenna (dotted line), as a function of incidence angle for and ascending tracks of data within Cycles 132 (left panel) and 137 (right panel). These Cycles correspond to the least negative (-0.47 dB) respectively most negative (-0.93 dB) average ratio within the period July 2007 to June 2008. The thin lines indicate the error bars on the estimated mean.*

statistics very sparse.

21 August 2003 - 30 June 2008 (Cycle 88 to 137)

On 21 August 2003, the public dissemination of UWI data is restarted. This fortunate event makes an end to the restricted distribution. From this date onwards data is received in the original manner (via the UK Met-Office), and is stored in the usual ECMWF analysis-input archives (the restricted data had been archived at a less accessible location). The original monitoring in the assimilation system (e.g., comparison with FGAT winds) is restored. However, cyclic reports are still based on the off-line monitoring (FG winds), since it includes data that is rejected in an early stage of the assimilation system. Besides Kiruna station, data is now also received from Maspalomas, Gatineau and Prince Albert, which, bearing in mind the loss of the LBR recorders, results in a coverage over the North Atlantic, part of the Mediterranean, the Gulf of Mexico, and a small part of the Pacific north-west from the US and Canada. An initial gap in the North Atlantic is resolved on 15 January 2004, when a station at West Freugh (Scotland) is included. Coverage in the Caribbean is obtained by a station at Miami (February 2005), in the Chinese Sea by a station at Beijing (July 2005), and partial coverage over the Southern Hemisphere by the inclusion of McMurdo (Antarctica, June 2005) and Hobart (Tasmania, February 2006) stations, coverage over the Bay of Bengal and the North-Eastern part of the Indian Ocean by a station in Singapore (October 2006), and coverage of an area around South Africa by the inclusion of a station at Johannesburg on 23 May 2008. Between 8 March and 1 October 2007 no data from Hobart has been acquired because of an anomaly of the ground station antenna. From Beijing, no data was received between 23 February and 15 May 2008, and since then coverage has been sporadic. Between 7 April and 25 June 2008 data has been missing from Miami caused by a lightning strike. The areas covered by Miami and Beijing station allow for the accurate observation of a number of tropical cyclones. For Cycle 137, the joining together of all available ground stations leads to a coverage as indicated in Figure 17.

The recording by separate ground stations means that in certain areas observations are reported more than once. For each ground station, gridding into 25-km cells and de-aliasing is performed separately. It is found that overlapping cells may be dislocated (by 12.5 km), and that regularly not the same wind solution is selected for all ground stations. The de-aliasing software that is responsible for this selection, acts on patches of UWI data. For data in overlapping regions (which are usually located around the border of the ground station visibility) different patches have been used for different stations, which explains the occasional difference in chosen wind

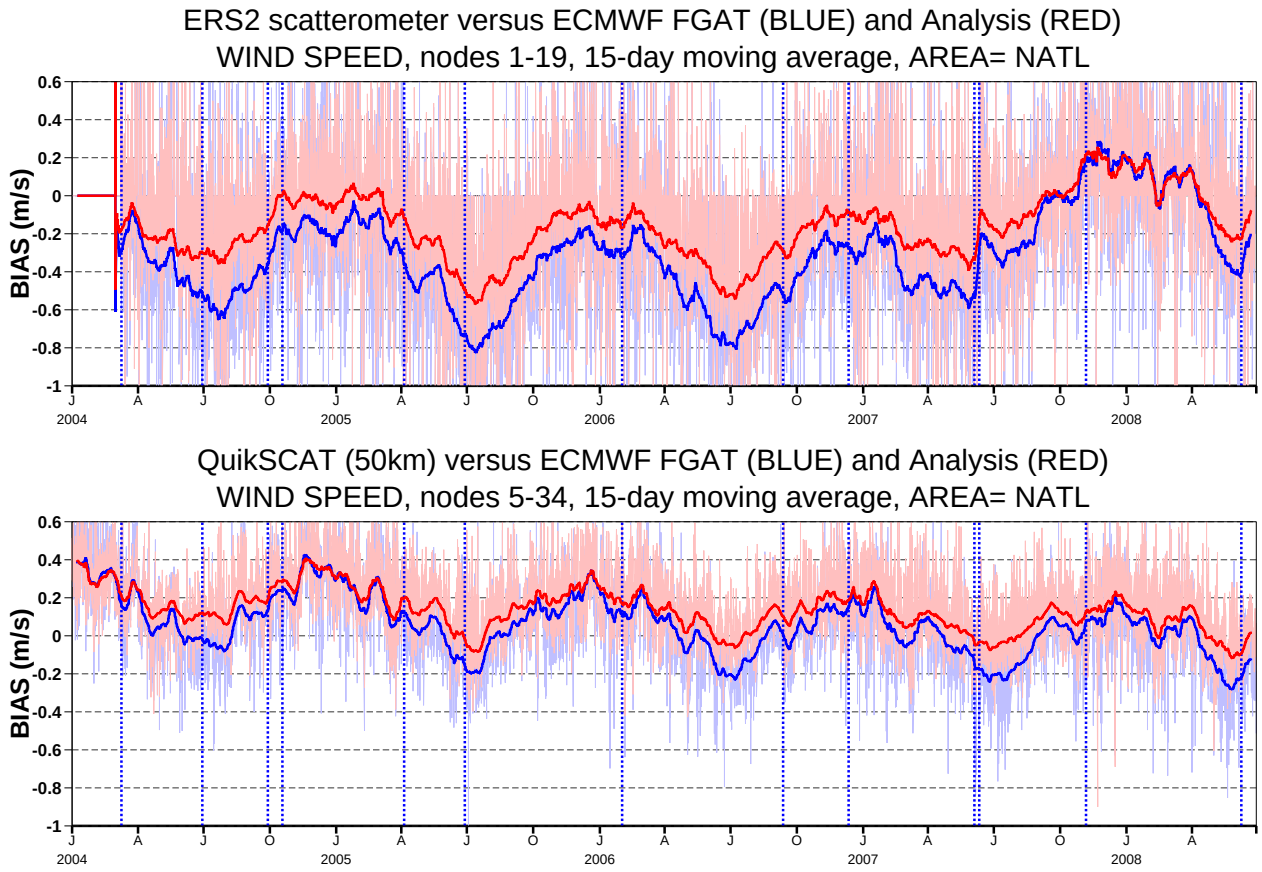

Figure 19: Wind-speed bias relative to FGAT winds for actively assimilated ERS-2 winds (based on CMOD5 before 7 June 2007; CMOD5.4 afterwards) for nodes 1-19 (top panel) respectively 50-km QuikSCAT (based on the QSCAT-1 model function and reduced by 4%) for nodes 5-34 (lower panel), averaged over the area (20N-90N, 80W-20E), and displayed for the period 01 January 2004 - 30 June 2008. Fat curves represent centred 15-day running means, thin curves values for 6-hourly periods. Vertical dashed blue lines mark ECMWF model changes.

solution.

The operational ESACA processor has resolved all non-optimal features that had been detected during the validation period. Data quality is found to be high, although the cone distance has increased and is now 10% higher than for nominal data (see top panel of Figure 16). Assimilation experiments with winds inverted on the basis of CMOD5 show a small positive impact in global forecast skill (Hersbach *et al.* , 2004). It leads to the re-introduction of ERS-2 scatterometer data in the ECMWF assimilation system on 8 March 2004.

An original flag for high k_p values is now also set for yaw attitude errors exceeding 2 degrees. It appears to work well and a close correlation with the asymmetry in incidence angle is observed. It is routinely checked whether peaks in attitude errors coincide with enhanced solar activity. Magnetic storms influence the outer part of the atmosphere, which in turn could affect the ERS-2 platform. Although sometimes collocations between anomalies and solar storms occur, the relation is not obvious. Besides, since mid 2006 the Sun resides near the minimum of its (chaotic) 11-year solar cycle, and, as a result, magnetic storms have been relatively sparse.

Since the loss of global coverage, a seasonal trend has been introduced in the now regional data set, making objective monitoring more difficult. A clear example of such a trend is observed for the relative standard

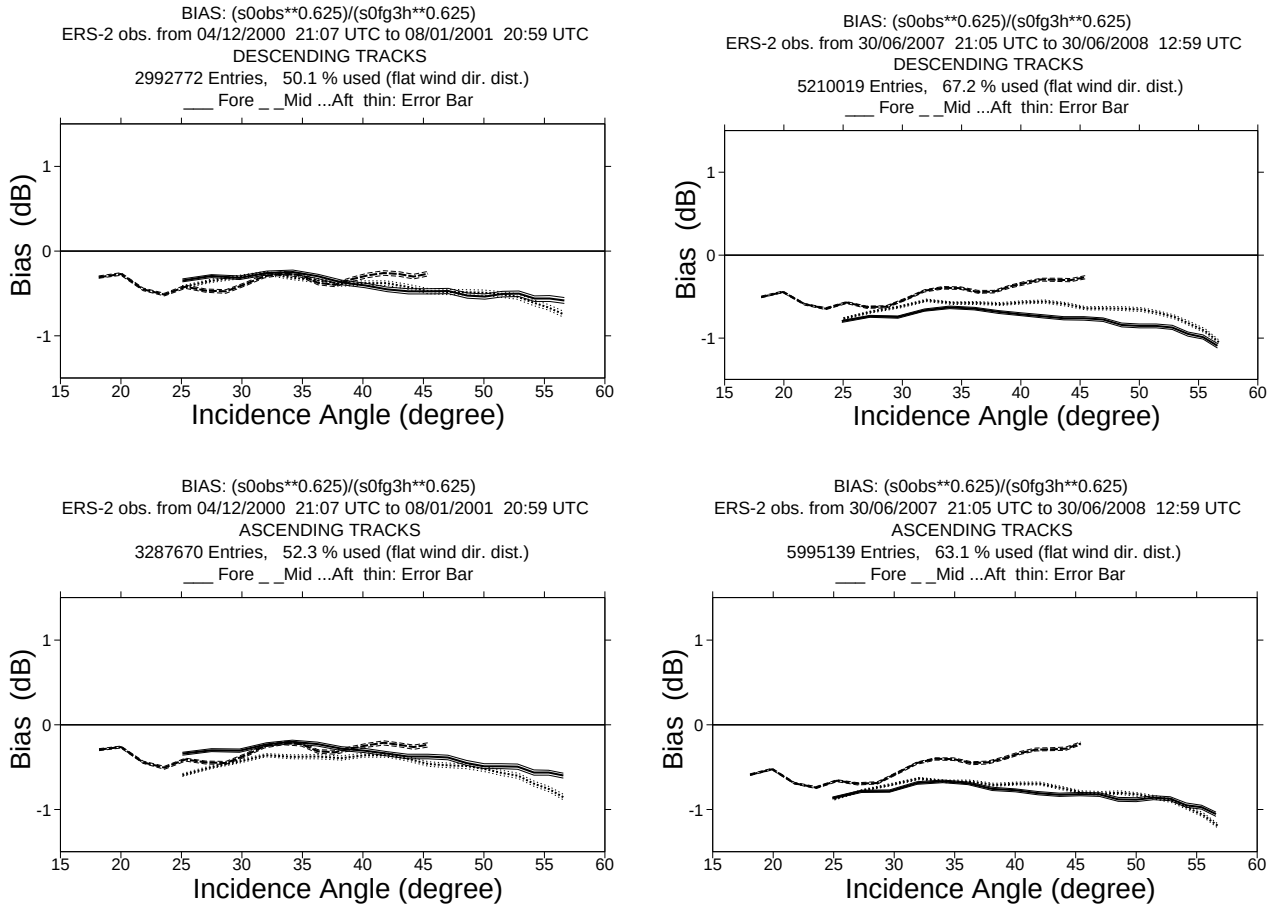

Figure 20: The same as Figure 18, but now averaged over Cycle 59 (left-hand panels) and the one-year period July 2007 to June 2008 (right-hand panels) for descending (top panels) respectively ascending (lower panels) tracks.

deviation of the UWI wind speed compared to FG winds (see second panel of Figure 16); a more intense and volatile wind climate in winter time will naturally lead to an increased RMSE.

A seasonal trend also appears for bias levels of both wind speed and backscatter. For backscatter, bias patterns are found to be flat in winter time, but large asymmetries emerge during summer. Typical examples for this consistent yearly trend are given in Figure 18. For wind speed, bias relative to ECMWF FG winds, are found to be (like backscatter) most negative around July ($\sim$ 1.1 m s^{-1}) and least negative around January ($\sim$ 0.7 m s^{-1}). The seasonal fluctuations are thought to be related to seasonal variations in the stability of the marine boundary layer. For a discussion, see Section 5.4 of Abdalla and Hersbach (2006). The same trend is observed for ERS-2 winds as assimilated at ECMWF. These are not based on CMOD4 (as the UWI product) but are inverted by the usage of CMOD5 before 7 June 2007, and CMOD5.4 afterwards. A time series of active ERS-2 data restricted by an area in the North Atlantic is displayed in the top panel of Figure 19. The lower panel shows the evolution of the bias of active QuikSCAT data (subject to the same area). It displays a similar yearly cycle, which confirms that the evolution in relative bias most likely has a geophysical nature, rather than being the result from a drift in the ERS-2 AMI instrument.

In order to filter out seasonal effects, relative biases in backscatter space are presented in (the right-hand panels of) Figure 20 for the one-year period July 2007 to June 2008. For Cycle 59 (end 2000) similar plots are presented in the left-hand panels. Although accumulated over the limited 5-weekly period for this Cycle,

seasonal effects are still filtered out by the fact that data was globally available (other cycles in 2000 display a similar pattern, not shown). Comparison between the two sets of plots shows that current bias levels are about 0.25 dB more negative than for nominal data. It is a reflection of the enhancement of ECMWF surface winds by about $0.3\,\mathrm{m\,s^{-1}}$ over the last 6 years. This trend emerges, e.g., from longterm monitoring of QuikSCAT winds and also buoy winds (not shown). The inter-antenna asymmetry has increased. For higher incidence angles the bias level of the mid antenna is less negative than for the other two antennas; especially for the ascending tracks. This asymmetry is most prominent during the Summer as can e.g., be seen from the right-hand panel of Figure 18. Its origin is not known.

For wind the accumulation over the one-year period July 2007 - June 2008 (and all 19 nodes), indicates that UWI winds are on average $0.9-1.0\,\mathrm{m\,s^{-1}}$ biased low compared to ECMWF FG winds (top left-hand panels of Figure 21). This is slightly more negative than for nominal data (before January 2001), and matches the gradual increase ($\sim 0.30\,\mathrm{m\,s^{-1}}$) in average wind speed of the ECMWF first-guess winds since 2000 as mentioned above. Compared to a yearly average from July 2006 - June 2007 (Figure 22), the situation is very stable. For both wind speed and wind direction, scatterplots with respect to ECMWF FG winds are quite similar. The main difference is a change in relative bias from $-0.87\,\mathrm{m\,s^{-1}}$ to $-0.95\,\mathrm{m\,s^{-1}}$. A similar bias evolution emerges for QuikSCAT data. It therefore, reflects an increase of the average ECMWF FG wind speed by about $0.1\,\mathrm{m\,s^{-1}}$, which is the result of several changes in the ECMWF operational system during 2007 and 2008. A similar picture holds for winds derived from CMOD5. Scatter plots for 2008 are, besides a small change in wind speed bias, similar to those for 2007. Average relative wind bias of CMOD5 is now around $-0.45\,\mathrm{m\,s^{-1}}$, which is on the level of the bias of CMOD5 compared to buoy data. In other words, ECMWF FG winds are now nearly unbiased with respect to buoy data.

Compared to the situation of nominal data (e.g., before 2001), the current one-year accumulated relative standard deviation of UWI winds is about 0.1 $\mathrm{m\,s^{-1}}$ lower (1.5 $\mathrm{m\,s^{-1}}$ versus 1.6 $\mathrm{m\,s^{-1}}$). It is difficult to state whether the quality of the UWI product has changed, since part of the lower STDV should be the result of the current omission of strong (e.g. volatile) winds in the Southern Hemispheric storm tracks, combined with a gradually improving quality of ECMWF winds.

As observed during the ESACA test phase, the quality of UWI wind direction is (as a result of the improved de-aliasing algorithm) superior to that of nominal data (see lower panel of Figure 16). Nevertheless, incorrect wind solutions are still frequently reported as can be seen from the lower panels of Figure 21. Occasionally, peaks of degraded performance have occurred (latest between 25-27 October 2007; see report for Cycle 130 for details), which usually can be traced back to temporarily missing input (model winds) in the ESACA de-aliasing software. Such peaks are not observed for at ECMWF de-aliased CMOD5 winds.

A previously non-existing bias is observed for wind direction. On average, (de-aliased) ERS-2 winds are found to be rotated by 2 to 3 degrees counter-clockwise compared to ECMWF first-guess fields. One reason for this consistent bias appears the lack of cross-isobar flow (Hollingsworth 1994) at warm advection of ECMWF surface winds. A similar, opposite, effect is found on the Southern Hemisphere, and, therefore, this bias is almost averaged out in a global verification, but not in an unequally distributed data set like for ERS-2. A study for QuikSCAT data versus model winds may be found in Brown *et al.* 2005.

Locations for large differences between UWI (or CMOD5) winds are usually isolated. They often indicate meteorologicaly active regions, for which UWI data and ECMWF model field show reasonably small differences in phase and/or intensity. Tropical cyclones and frontal systems are typical candidates. One example (left-hand panel of Figure 23) was a frontal system in the North Atlantic on 8 February 2008. Here, apart from an underestimation caused by CMOD4 and some de-aliasing problems, the UWI winds are probably more correct.

Besides large differences that pin point errors in the ECMWF first-guess field, occasionally cases are observed in which UWI winds seem clearly incorrect. This is often manifested as odd patches within a surrounding wind

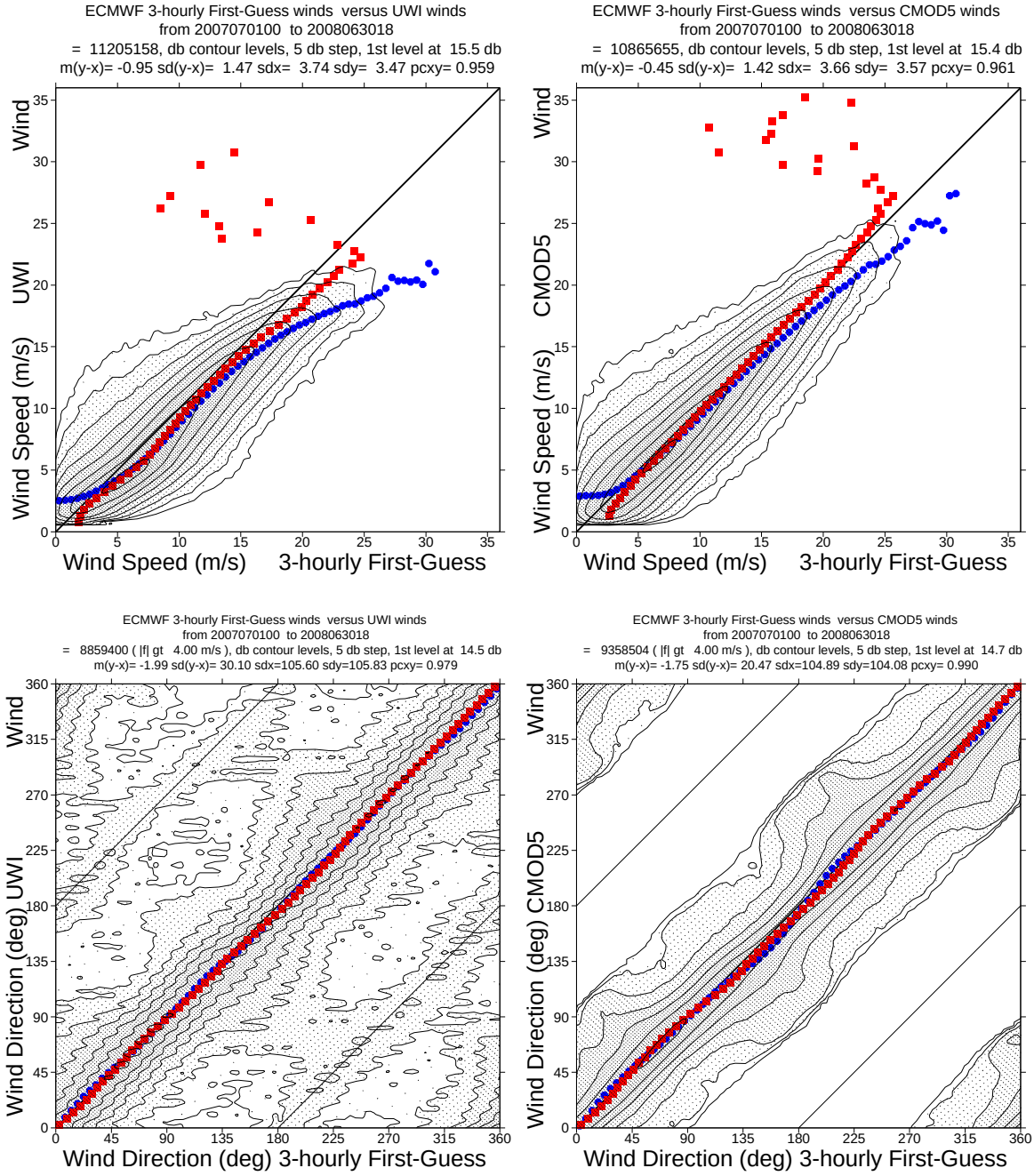

Figure 21: Two-dimensional histogram of UWI (left hand panels) and de-aliased CMOD5 (right hand panels) relative to ECMWF FG for wind speed (top panels) and wind direction (lower panels) over the one-year period from 1 July 2007 to 30 June 2008. Blue circles denote averages for bins in the x-direction, and red squares averages for bins in the y-direction.

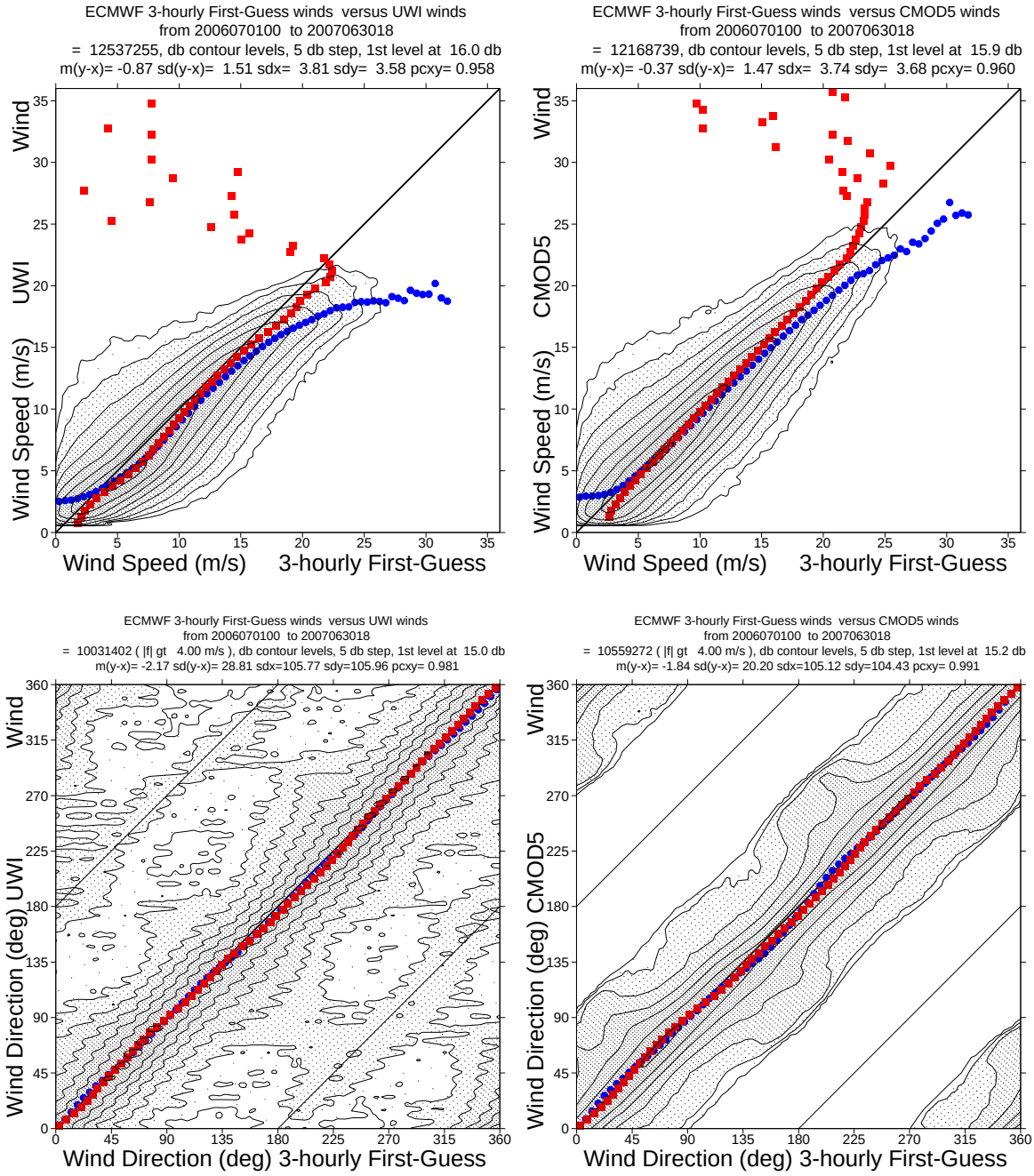

Figure 22: The same as Figure21, but now for the period 1 July 2006 - 30 June 2007.

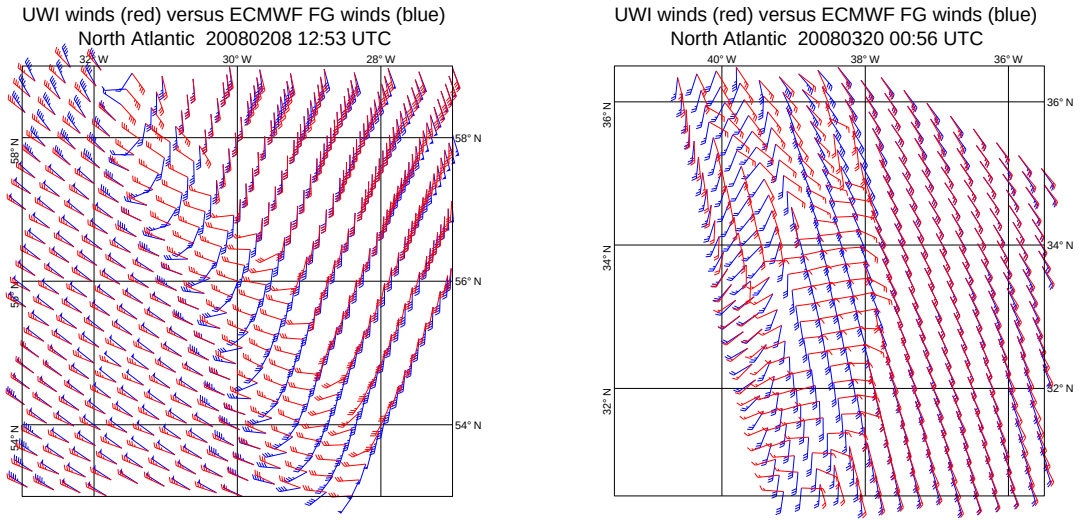

Figure 23: Two examples for situations where scatterometer and ECMWF winds differ significantly.

field of presumably good quality. An example is shown in the right-hand panel of Figure 23. Problems are found most likely to occur at light wind conditions relatively close to land, and at lower incidence angles in general.

4.4 CMOD5.N: a C-band geophysical model for equivalent neutral wind

From theoretical grounds, scatterometer backscatter should correlate most closely with surface stress. Since this quantity cannot be obtained accurately from in situ observations, in practice readily available winds at a standard height are used in scatterometer calibration studies, instead. As such, the CMOD5 model function is the result of a comparison of ERS-2 backscatter with ECMWF model wind at 10-m height. Typical variations in the relation between stress and surface wind mainly depend on atmospheric stability and ocean-wave sea state. In order to compensate for stability effects, the concept of (equivalent) neutral wind has been developed. Such neutral winds can be estimated from real winds (to be called non-neutral from now on) by transformation of such winds (at observation height) to surface stress by taking account of additional information on atmospheric stability, and subsequently transforming back by the neglect of these stability effects. On average, the marine boundary layer is weakly unstable, and at 10-metre height the global average neutral wind appears $\sim 0.2\,\mathrm{m\,s^{-1}}$ stronger than the non-neutral wind.

Ku-band model functions (NSCAT-1,2, QSCAT-1) have traditionally been tuned on neutral wind, rather than on non-neutral wind like the C-band CMOD model family (e.g., CMOD2, CMOD4, CMOD5). Since the first approach represents the most natural choice, a C-band model function for neutral wind has been established. This model function, called CMOD5.N, embodies a refit of CMOD5 in such a way that its 28 tuneable coefficients lead, for given backscatter observation, to an enhancement of $0.7\,\mathrm{m\,s^{-1}}$ in wind speed. This value is chosen to be independent on wind speed and incidence angle, and incorporates the average difference between neutral and non-neutral wind ($\sim 0.2\,\mathrm{m\,s^{-1}}$) and for the known bias of CMOD5 ($\sim 0.5\,\mathrm{m\,s^{-1}}$) when compared to buoy wind data.

Details on the evaluation and validation of CMOD5.N are not given in this document, but may be found in Hersbach (2008). The resulting set of retuned coefficients is presented in Table 1. The quality of the CMOD5.N

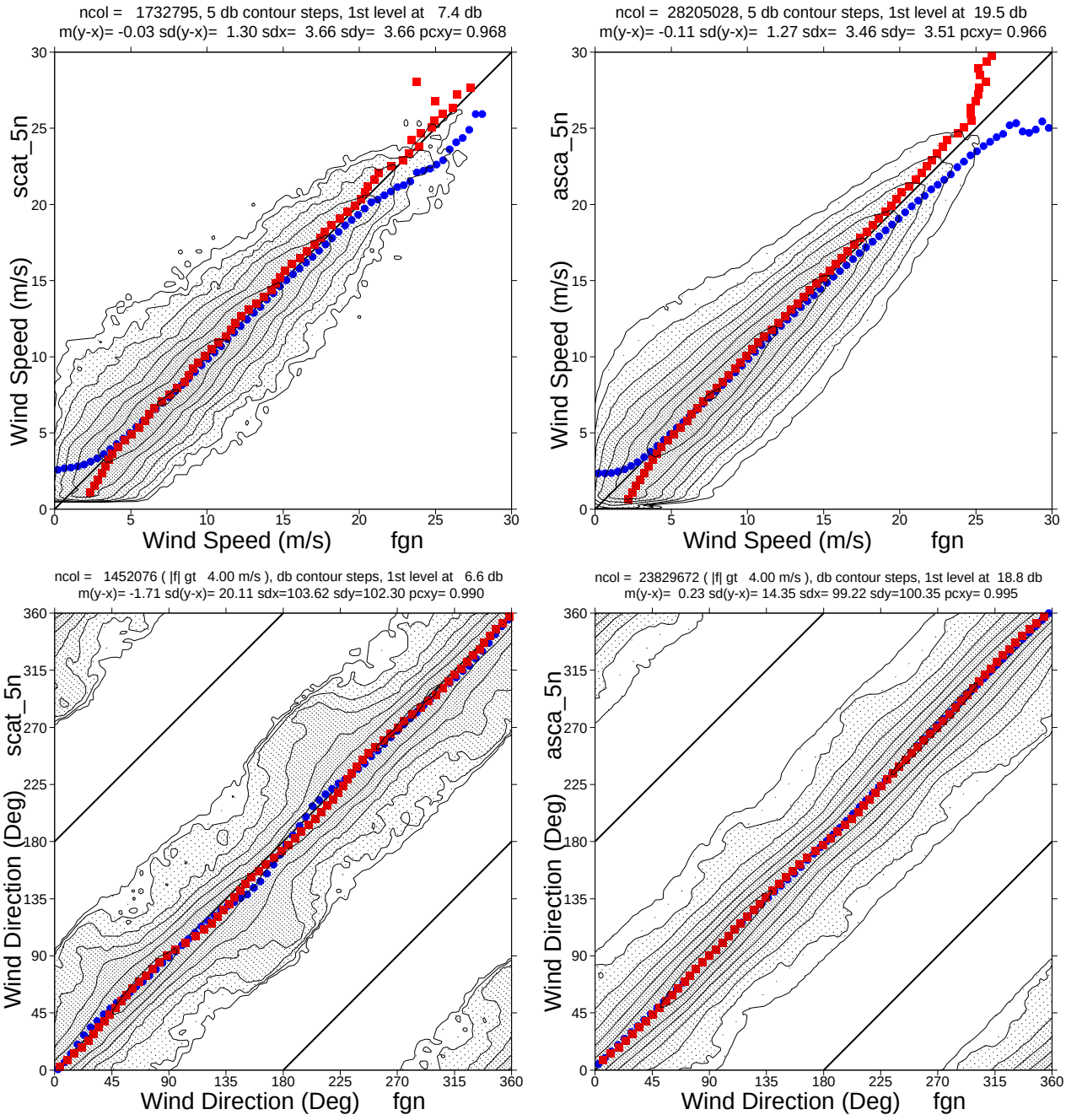

Figure 24: Scatter plot between ERS-2 wind (left) respectively ASCAT wind (right) based on CMOD5.N versus collocated ECMWF equivalent neutral short-range forecast wind at 10m. Top panel represents scatter diagrams for wind speed; lower panels for wind direction (for which both winds are at least $4 m s^{-1}$).

	CMOD5	CMOD5.N		CMOD5	CMOD5.N
c_1	-0.6880	-0.6878	c_{15}	0.0070	0.0066
c_2	-0.7930	-0.7957	c_{16}	0.3300	0.3222
c_3	0.3380	0.3380	c_{17}	0.0120	0.0120
c_4	-0.1730	-0.1728	c_{18}	22.000	22.700
c_5	0.0000	0.0000	c_{19}	1.9500	2.0813
c_6	0.0040	0.0040	c_{20}	3.0000	3.0000
c_7	0.1110	0.1103	c_{21}	8.3900	8.3659
c_8	0.0162	0.0159	c_{22}	-3.4400	-3.3428
c_9	6.3400	6.7329	c_{23}	1.3600	1.3236
c_{10}	2.5700	2.7713	c_{24}	5.3500	6.2437
c_{11}	-2.1800	-2.2885	c_{25}	1.9900	2.3893
c_{12}	0.4000	0.4971	c_{26}	0.2900	0.3249
c_{13}	-0.6000	-0.7250	c_{27}	3.8000	4.1590
c_{14}	0.0450	0.0450	c_{28}	1.5300	1.6930

Table 1: CMOD5 and CMOD5.N coefficients

refit has been tested for ERS-2 and ASCAT for the two one-month periods of July 2007 and January 2008. From this it is found that winds inverted with CMOD5.N are on average $0.69\,\mathrm{m\,s^{-1}}$ stronger than winds determined from CMOD5. As function of wind speed and incidence angle, fluctuations are well within $0.05\mathrm{m\,s^{-1}}$, and differences in wind direction appear small.

ASCAT and ERS-2 wind speed obtained from CMOD5.N compares on average well with ECMWF equivalent neutral FG wind. In comparison with non-neutral wind, local, seasonally dependent biases between scatterometer and ECMWF model appear reduced (Hersbach, 2008). An example is presented in Figure 24 for the above quoted two-months period. The relative bias is low and the difference in bias between ERS-2 and ASCAT is probably the result of a difference in sampling (non-global respectively global) as will emerge in Section 4.5. The relative standard deviation in wind speed is comparable between ERS-2 and ASCAT. For wind direction, however, ASCAT clearly outperforms ERS-2. Besides a lower STDV (14.4 degrees compared to 20.1 degrees for ERS-2), the scatter plot looks homogeneous. It does not contain a s-shape as is visible for ERS-2. This non-optimal feature for ERS-2 may be the result of a calibration issue of the mid beam compared to the fore and aft beam, as e.g. visible in Figure 20. The s-shape may be resolved by a bias correction of the mid beam prior to wind inversion.

4.5 Collocation of ERS-2 data with ASCAT data

On 12 June 2007, data from the ASCAT scatterometer on-board MetOp-A was introduced in the operational assimilation suite at ECMWF. Winds are, like ERS-2 from this date onwards, based on CMOD5.4. Due to a difference in calibration between ERS-2 and ASCAT, bias corrections in backscatter space and wind speed before respectively after wind inversion are applied (see Hersbach and Janssen, 2007 for details). The resulting ASCAT wind product is unbiased to ECMWF FG wind speed. The same is true for the ERS-2 scatterometer product once seasonal effects have been filtered out (see .e.g. the right-hand panels in Figure 21 for winds based on CMOD5 = CMOD5.4 - $0.48\mathrm{m\,s^{-1}}$). Therefore, ERS-2 and ASCAT should be well calibrated with respect to one other, which is a desirable requirement when both are assimilated simultaneously.

An illustration of this is presented in Figure 25,which shows the observation of an intense low near the British Isles by ASCAT and ERS-2 around 00 UTC 9 December 2007. It contains three tracks for ERS-2 and three for

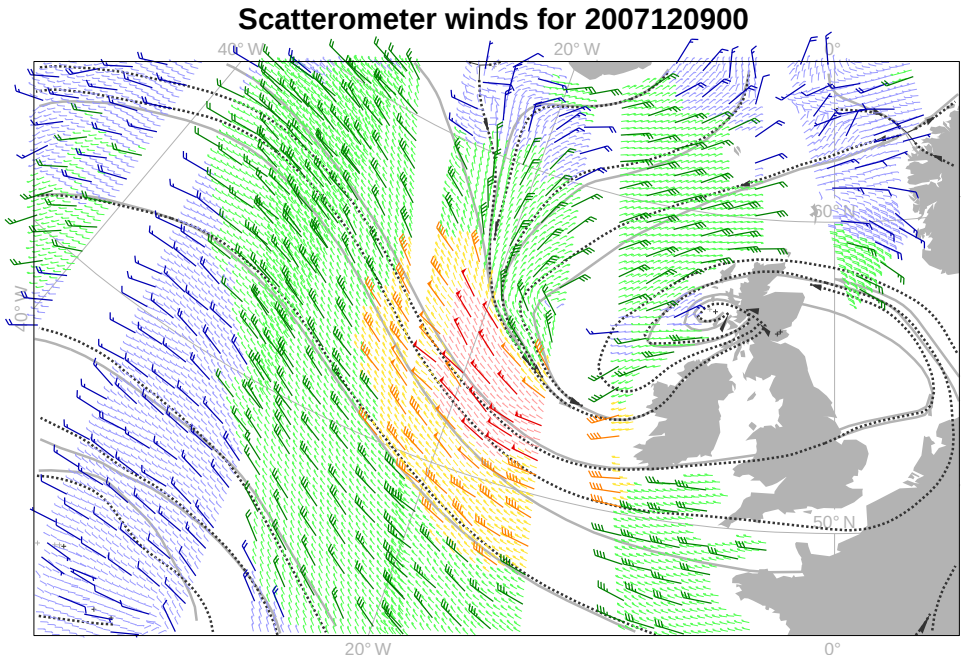

Figure 25: Scatterometer winds from ERS-2 and ASCAT as assimilated at ECMWF for the 12-hour assimilation cycle of 00 UTC 9 December 2007. The two tracks around 40W and the track parallel to 10W concern ASCAT data; the three tracks around 45W, 20W and 0W originate from ERS-2. Large barbs indicate actively assimilated winds and small barbs indicate rejected (mostly thinned) winds. Colors indicate speed ranges (blue less than $10ms^{-1}$, green 10-$20ms^{-1}$, orange 20-$25ms^{-1}$, and red exceeding $25ms^{-1}$). Black and grey lines represent streamlines for the ECMWF analysis and first-guess surface winds.

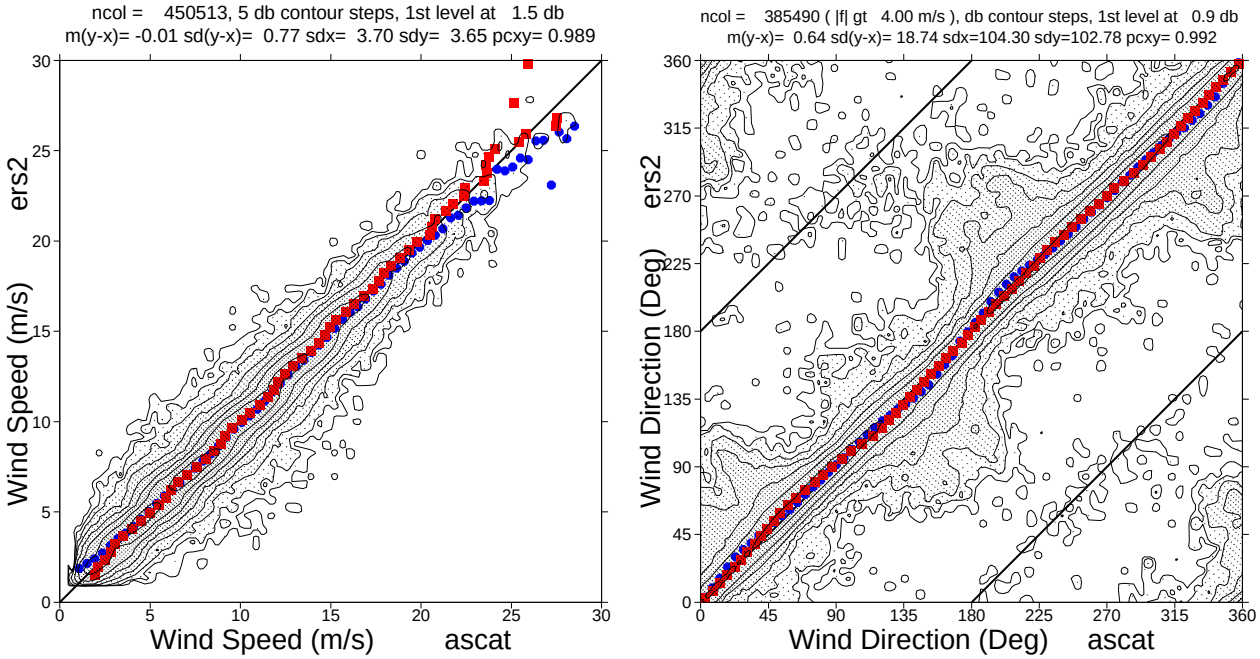

Figure 26: Scatter plot between ASCAT wind and ERS-2 wind as assimilated at ECMWF for the period July 2007 - June 2008, and where both observations are less than 25km and 30 minutes apart in space and time. Left panel represents wind speed; right panel wind direction (for which both winds are at least $4ms^{-1}$).

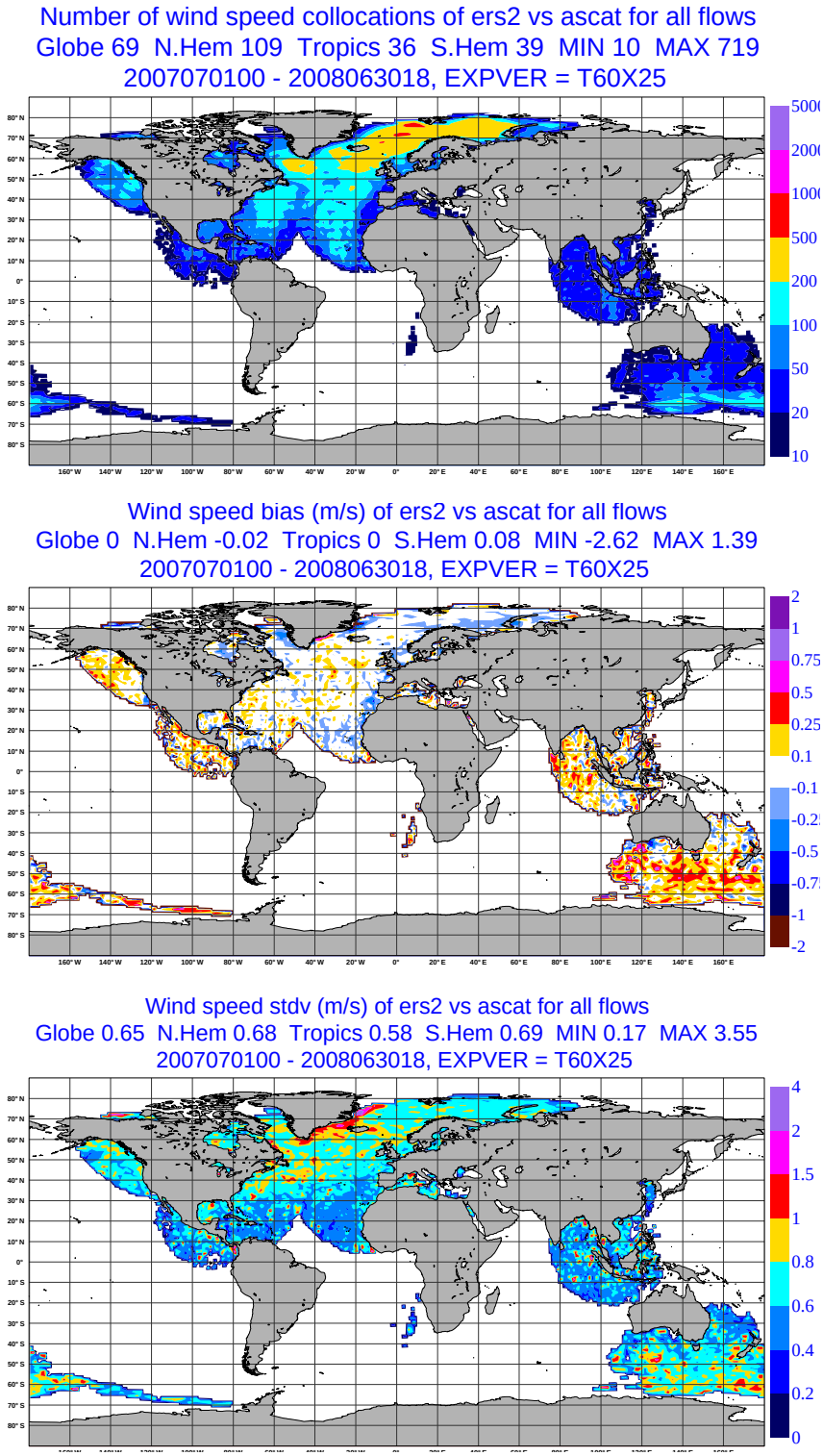

Figure 27: Number (top) of collocations per N80 reduced Gaussian grid box (∼ 125 km), relative bias (middle) respectively standard deviation (lower panel) (∼ 125 km) of ERS2 versus ASCAT wind speed, where both observations are less than 25km and 30 minutes apart in space and time within the period July 2007 and June 2008. Results are only plotted for grid cells that contain at least 10 observations.

ASCAT (details are given in the Figure caption). As a result of the appropriate inter-calibration it is difficult to spot which track originates from what instrument. Therefore, the analysis system is presented with two consistent data sets, and the detailed combined information on the low pressure system can be fully exploited.

Thanks to the similar ascending node time for the ERS2 and Metop-A satellites, both scatterometer tracks are in general not too far apart. In some situations, like for the case in Figure 21, swaths are shifted, and in return a synergetic detailed picture of the surface wind field is obtained. In other situations, tracks overlap, which allow for an accurate cross-validation between both scatterometer instruments.

At ECMWF, a collocation effort has been initiated. For this, all observations are searched for which ERS-2 and ASCAT data are sufficiently close in space and time. A resulting scatter plot of ERS-2 and ASCAT collocations is presented in Figure 26. Here limits of 25km in location and 60 minutes in time have been imposed for the one-year period July 2007 - June 2008. All ERS-2 data that had passed the screening process at ECMWF were taken into consideration. This includes in principle data from all 19 WVC's, but excludes e.g., data over land and for which the combined k_p-yaw flag had been set. For technical reasons for ASCAT, only at ECMWF actively assimilated, thinned data could be selected (only 12 out of 42 WVC's). Also for technical reasons, for each instrument only the wind ambiguity closest to the ECMWF FGAT vector wind was regarded. Both limitations may be relaxed in the future. The data coverage and number of collocations are displayed in the top panel of Figure 27. Comparison with the general data coverage of ERS-2 (see e.g. as indication Figure 17) shows that ERS-2 and ASCAT basically collocate in all locations where ERS-2 data is available.

The left-hand panel of Figure 26 confirms the consistency between ERS-2 and ASCAT wind speed. An overall relative bias seems absent, and as function of wind speed no clear biases are visible. The scatter in wind speed is remarkably low. Its value of only $0.77\,\mathrm{m\,s^{-1}}$ is much lower than the scatter between scatterometer and model wind ($\sim 1.2-1.4\,\mathrm{m\,s^{-1}}$). In case collocation criteria are narrowed down, an even somewhat lower scatter is obtained (not shown). A reason for the low scatter is that both instruments share the same observation principle over a similar spatial area. Therefore, representation and systematic errors hardly contribute. The largest source of scatter is probably the instrument noise of each scatterometer observation. In case it is assumed that the noise levels of ASCAT and ERS-2 are similar, each instrument has a random error of around $0.5\,\mathrm{m\,s^{-1}}$ in wind speed.

Although the average wind speed bias is very small, locally biases do exist (middle panel of Figure 27). Some biases appear where statistics is low, and are for that reason probably not significant. For the strong winds in the storm track south of Australia, where data coverage is much higher, the higher ERS-2 wind speed may indicate a small relative bias for the more extreme situations. The lower panel of Figure 27 gives the geographical distribution of the STDV between ERS-2 and ASCAT wind speed. An array of bullet points of locally enhanced values indicates isolated cases where large differences between both scatterometers occurred. Some may be the result of occasional instrument anomalies. A larger area of scatter is found for a region south of Greenland.

For wind direction, the comparison between ERS-2 and ASCAT is less favourite, as can be seen from the right-hand panel of Figure 26. A number of nearly anti-parallel collocations is likely the result of the limitation in the choice of the wind solution (closest to ECMWF FGAT wind), which is to be resolved when a comparison between all ambiguities is performed. The s-shape structure is to be attributed to a non-optimality for ERS-2, since a similar structure is present in a comparison of ERS-2 versus ECMWF wind, while absent in a comparison between ASCAT and ECMWF wind (see e.g., lower panels of Figure 24).

The regional coverage of ERS-2 has introduced a seasonal dependence in the monitoring with respect to ECMWF wind. It is interesting to investigate whether such a cycle also exists for a comparison with ASCAT data. Time series for the relative bias and STDV for ERS-2, ASCAT and ECMWF winds for collocated data are presented in Figure 28. The comparison of ERS-2 (blue) and ASCAT (red) with ECMWF FGAT wind shows the characteristic seasonal trend of stronger scatterometer winds in winter, and weaker in summer, with an amplitude of around $0.4\,\mathrm{m\,s^{-1}}$ Such a trend is hardly visible for the comparison between ERS-2 and ASCAT.

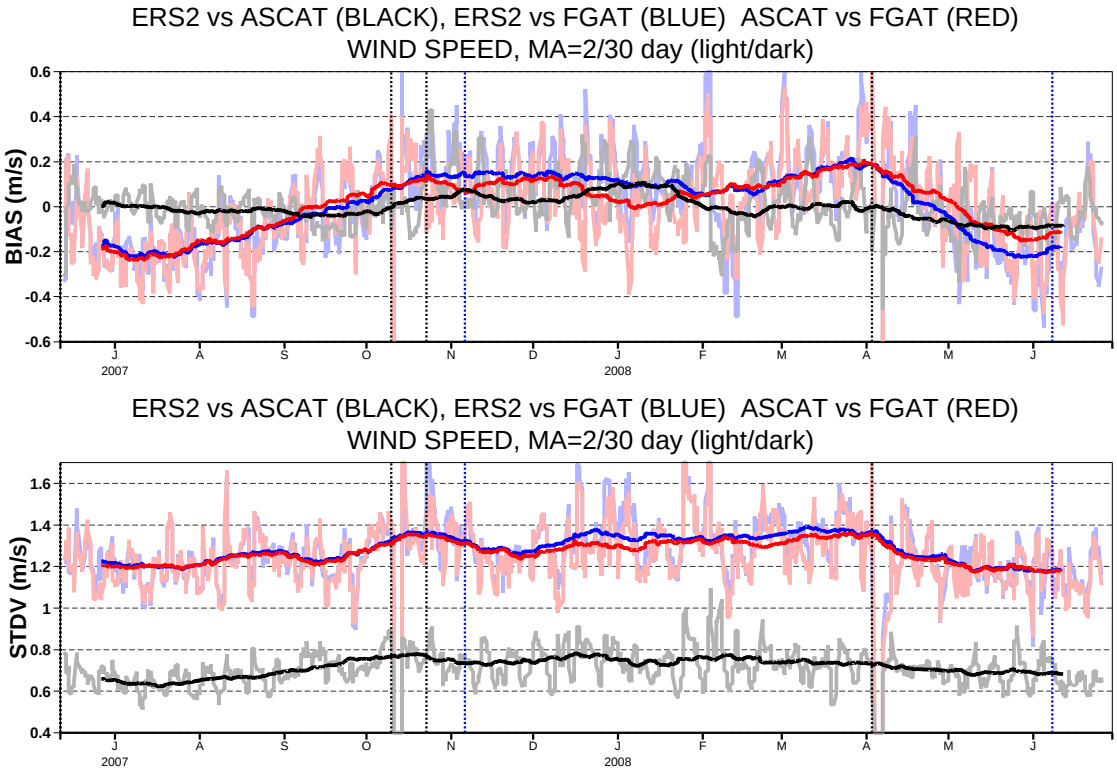

Figure 28: Time series of the relative bias (top panel) and standard deviation (lower panel) in wind speed between ERS2 and ASCAT (black), ERS2 and ECMWF FGAT (blue), ASCAT and FGAT (red) for situations in which ASCAT and ERS2 observations are closer than 25km and within 30 minutes. Vertical dotted lines mark changes in the ECMWF operational system (blue) or updates in the ASCAT calibration (black).

This confirms that the drift in bias between scatterometer data and model data has a geophysical nature rather than being a drift in the scatterometer calibration. The time evolution of the relative bias between ERS-2 and ASCAT can detect a drift in calibration for each instrument. So far, the trend in the relative bias is within $0.2\,\mathrm{m\,s^{-1}}$. Although there is no clear seasonal trend in the relative bias between both scatterometers, there is a trend in the STDV. This is most likely the reflection of the yearly variation of the wind climate. In winter, when wind speed is higher, STDV is slightly larger than in summer. It indicates that the scatterometer random error in wind speed slightly scales with wind speed.

5 Concluding remarks

Continuous monitoring and verification of the ERS-2 fast delivery wind and wave products from RA (URA), SAR (UWA) and scatterometer (UWI) are carried out routinely at ECMWF. Data from ECMWF atmospheric (IFS) and wave (ECWAM) models and from in-situ buoy observations are used for this purpose. As a result of the loss of gyros in early 2001, several products were degraded. The main victim was the UWI product, which became of poor quality forcing ESA to halt its dissemination. ESA managed to improve the quality of the UWI product which culminated in the public re-dissemination on 21 August 2003. The quality of the UWI product has been closely monitored at ECMWF since 12 December 2001. On 8 March 2004 ERS-2 scatterometer data was reintroduced at the ECMWF assimilation system. The degradation impact of zero-gyro mode was less pronounced on the URA and UWA products. Since the failure of the ERS-2 low bit rate tape recorders on 22

June 2003, data coverage has been restricted within the visibility of ground stations covering the North Atlantic and western coasts of North America. More ground stations were later utilized to extend the coverage to the Southern Ocean, the eastern coasts of China, the northeastern parts of Indian Ocean and the southern coasts of Africa. Despite the lack of the global coverage of LBR ERS-2 data, the remaining coverage represents an important area for many applications. Even positive impact on global forecast skill was found in several assimilation experiments (Hersbach, 2004), which led to the re-introduction of the usage of ERS scatterometer data at ECMWF on 8 March 2004. Among others, for these reasons maximum possible continuation of the ERS-2 mission is important.

The SAR radar incident angle, as reported in the UWA product, has been unstable (i.e. varies between 16.3° and 26.5°) recently. Until the 5th. of February 2008, the incidence angle used to vary within a fraction of a degree around the nominal value of 23°.

Long-term evaluation of ERS wind and wave products was carried out for the whole lifetimes of both ERS-1 and ERS-2 missions. Offline altimeter ocean product (OPR) and fast delivery products from SAR (UWA) and scatterometer (UWI) were evaluated (for full details refer to Abdalla and Hersbach, 2006 and 2007) and the following results were obtained:

- OPR SWH products from both satellites are of good quality. ERS-2 SWH product is about 30 cm higher than ERS-1. It seems, however, that ERS-1 SWH product is slightly better than ERS-2 product.
- The OPR wind speed product had several problems by time. ERS-1 OPR wind product suffered significant abrupt changes in bias at least 3 times. On the other hand, ERS-2 OPR wind speed product was rather stable for the first 4.5 years before it started to degrade (especially in the Southern Hemisphere) after the gyro problems started in early 2000. Therefore, one should handle the altimeter wind speed product with care especially for climate studies.
- SWH from ERS-1 UWA product is too high with respect to the wave model with at least two significant jumps in bias. The product seems to be degraded during Phase G (after March 1995). On the other hand, ERS-2 UWA product seems to be much better with lower bias and standard difference with respect to the wave model. However, a calibration bug (July 1998-November 2000) and the loss of the gyros (January-June 2001) degraded the product (or its inversion) during most of ERS-2 lifetime.
- A re-calibration of the ERS archive from the start until January 2001 on the basis of a collocation with ERA-40 (Uppala *et al.*) winds suggests that there is a small difference in calibration between ERS-1 and ERS-2 (Abdalla and Hersbach, 2007). Backscatter levels of ERS1 are around 0.2 dB higher than for ERS-2, which translates to a difference in wind speed of approximately $0.2\,\mathrm{m\,s^{-1}}$.
- The potential quality of the AMI wind product is stable and comparable between ERS-1 and ERS-2. Changes in the behaviour of the ERS-1 and ERS-2 UWI wind product can be attributed to changes in calibration of the underlying level 1B backscatter product (Abdalla and Hersbach, 2007). By bias-correcting level 1b values before wind inversion, it appears possible to obtain an unbiased wind product of consistent high quality for all incidence angles from 15 April 1992 for ERS-1 and from 22 November 1995 for ERS-2 onwards. This analysis, therefore, indicates a high potential for a re-processing enterprise, which should result in a homogenous, unbiased high-quality wind product for the entire ERS archive.

A collocation study between ERS-2 AMI data and ASCAT data from the MetOp-A satellite confirms that both the ERS-2 and ASCAT scatterometer are stable. In contrast to a comparison to ECMWF first-guess wind, hardly any seasonal trend is visible. Therefore, the collocation of data from both instruments together with ECMWF model data, provides a powerful tool to monitor the behaviour of each these three wind sources.

Monthly or cyclic monitoring reports can be found at:
URA (monthly): http://earth.esa.int/pcs/ers/ra/reports/ecmwf
UWA (monthly): http://earth.esa.int/pcs/ers/sar/reports/ecmwf (password protected)
UWI (5-weekly): ftp://earth.esa.int/pub/SCATTEROMETER/ecmwf_rep

Acknowledgements

The work presented in this paper was funded by ESRIN (Project Ref. 18212/04/I-OL). We would like to thank Peter Janssen, Jean-Raymond Bidlot, Lars Isaksen and Raffaele Crapolicchio, for support and valuable discussions.

A Appendix: Related Model Changes

Note: All changes were introduced for the 6-hour time-window centred at 18:00 UTC.

21 Jun. 1992 Operational implementation of the global model on a 3 degree latitude-longitude grid (63°S to 72°N). The wave spectrum is discretized using 12 directions and 25 frequencies (from 0.041772Hz).

15 Aug. 1993 Assimilation of ERS-1 RA wave heights in global model.

3 Jul. 1994 The global model horizontal resolution was increased to 1.5 degree (from 81°N to 81°S).

19 Sep. 1995 New windsea/swell separation scheme.

30 Jan. 1996 Changes to IFS (e.g. 3DVAR operational).

1 May 1996 Assimilation switch from ERS-1 to ERS-2 RA wave heights.

1 Jun. 1996 Changes to IFS to switch the assimilation of scatterometer winds from ERS-1 to ERS-2.

4 Dec. 1996 The global model horizontal resolution was changed to a 0.5 irregular latitude-longitude grid, with an effective resolution of about 55 km (from 81^oN to 81^oS). Change the wave-model integration scheme to accommodate Hersbach and Janssen new limiter.

13 May 1997 Modification of the advection scheme by defining the first direction as half the directional bin.

27 Aug. 1997 Changes to IFS (e.g. scatterometer winds are no longer blacklisted for speeds above 20 m/s and modification to the scatterometer bias).

11 Nov. 1997 Changes to IFS (e.g. modification of the scatterometer QC).

25 Nov. 1997 Changes to IFS to implement the 4D-Var assimilation scheme.

1 Apr. 1998 Changes to IFS model (e.g. change horizontal resolution to T319).

28 Jun. 1998 Operational implementation of the coupling between WAM and IFS.

9 Mar. 1999 10 m winds are used in coupled model. IFS changes (e.g. change vertical resolution to 50 levels, and modification of the scatterometer QC).

13 Jul. 1999 RA wave height correction based on non-gaussianity of the sea surface elevation. Change to the frequency cut-off in the integration scheme. IFS changes (new physics/dynamics coupling).

12 Oct. 1999 Changes to IFS model (e.g. change vertical resolution to 60 levels, and new orography)

11 Apr. 2000 RA data quality control based on peakiness factor. Penalization of low altimeter wave heights in data assimilation. An extra iterative loop to determine the surface stress.

27 Jun. 2000 Sea ice fraction is used for the ice mask. The buoy validation software was upgraded to use the proper anemometer height.

11 Sep. 2000 Assimilation scheme in IFS changed to 12 hour 4D-Var.

20 Nov. 2000 Increase the horizontal resolution of the atmospheric model to T511 (around 40 km). Increase spectral resolution in the global deterministic WAM model to 24 directions and 30 frequencies. Improved advection scheme on irregular grids. New empirical growth curves in the RA data assimilation. Bug fix of the SAR inversion software to properly use SAR data with the new calibration procedure (the bug was effective since June 1998).

11 Jun. 2001 IFS modifications.

21 Jan. 2002 Modified scheme for the time integration of the source terms. Assimilation of QuikSCAT data in IFS model.

8 Apr. 2002 Inclusion of wind gustiness and air density effect. Removal of spurious values for the Charnock parameter. Blacklisting procedure for wave data.

16 Apr. 2002 Extra quality control for QuikSCAT.

13 Jan. 2003 Assimilation of ERS-2 SAR data. Background check for altimeter data during assimilation. Significant changes to IFS model, including a new minimisation scheme and improved background error in the assimilation part.

22 Oct. 2003 Assimilation of ENVISAT Radar Altimeter-2 Ku-Band significant wave heights. ERS-2 RA wave height assimilation was discontinued. (This change was introduced at 6-hour time-window centred at 00:00 UTC.)

8 Mar. 2004 Use of unresolved bathymetry in wave model. Wave model is now driven by neutral 10-metre wind. Re-introduction of ERS-2 scatterometer data based on CMOD5.

28 Jun. 2004 The implementation of the early delivery system.

27 Sep. 2004 Proper treatment of the initialisation of wave fields for time windows 06:00 and 18:00 UTC.

5 Oct. 2004 Stop erroneously discarding some ENVISAT altimeter data in wave analysis.

5 Apr. 2005 Implementation of a revised formulation for ocean wave dissipation due to wave breaking.

1 Feb. 2006 Implementation of the high resolution atmospheric (T799) and wave (0.36°) models. ENVISAT ASAR Level 1b Wave Mode spectra replaced ERS-2 SAR in assimilation. Jason altimeter wave height data are assimilated.

12 Sep. 2006 Revised cloud scheme, including treatment of ice supersaturation and new numerics; implicit computation of convective transports.

5 Jun. 2007 Three outer loops for 4D-Var (T95/159/255).

12 Jun. 2007 Active use of IASI and ASCAT from METOP.

6 Nov. 2007 Atmospheric model changes including a new formulation of convective entrainment and relaxation timescale.

3 Jun. 2008 Atmospheric model changes. Improved advection scheme for wave model. Use of 4 wind solutions for QuikSCAT rather than 2 previously.

References

Abdalla S. and Hersbach H. (2006). The technical support for global validation of ERS Wind and Wave Products at ECMWF (April 2004 - June 2006), *Final report for ESA contract 18212/04/I-LG, ECMWF, Shinfi eld Park, Reading*.
http://www.ecmwf.int/publications/library/ecpublications/_pdf/esa/ESA_abdalla_hersbach_18212.pdf

Abdalla S. and Hersbach H. (2007). The technical support for global validation of ERS Wind and Wave Products at ECMWF (April 2004 - June 2007), *Final report for ESA contract 18212/04/I-OL, ECMWF, Shinfi eld Park, Reading*.
http://www.ecmwf.int/publications/library/ecpublications/_pdf/esa/ESA_abdalla_hersbach_18212-2007.pdf

Attema, E., P., W. (1986). An experimental campaign for the determination of the radar signature of the ocean at C-band, *Proc. Third International Colloquium on Spectral Signatures of Objects in Remote Sensing*, Les Arcs, France, ESA, *SP-247*, 791-799, 1986.

Brown, A. R., Beljaars, A. C. M., Hersbach, H., Hollingsworth, A., Miller, M., Vasiljevic, D. (2005). Wind turning across the marine atmospheric boundary layer *Quart. J. Roy. Meteor. Soc.* **607,** 233-1250.

ESA (2005). ERS-1 Mission Phases (from 1991 onwards). *An Internet web page* accessible from:
http://earth.esa.int/rootcollection/eeo/ERS1.1.7.html
Last visited: 21 July 2006.

Féménias P., and Martini A. (2000). ERS-2 AOCS mono-gyro attitude software Qualification Period - Radar Altimeter Data Analysis. *ESA-ESRIN Technical Note*, accessible from:
http://earth.esa.int/pcs/ers/ra/events/monogyro/

Hersbach, H. (2003). CMOD5. An improved geophysical model function. *ECMWF Technical memorandum* **395**, ECMWF, Reading, England.

Hersbach H., Janssen P. A. E. M., Isaksen, L. (2004). Re-introduction of ERS-2 scatterometer data in the operational ECMWF assimilation system. Procedings of the ENVISAT and ERS Symposium, Salzburg, Austria, 6-10 September 2004.

Hersbach H., Stoffelen A., and Haan de S., 2007, An improved C-band scatterometer ocean geophysical model function: CMOD5, *J. Geophys. Res., 112 (C3) C03006*.

H. Hersbach and P. Janssen, 2007. Preparation for assimilation of surface-wind data from ASCAT at ECMWF. *ECMWF Research Department Memorandum* **R60.9/HH/0750** Available from ECMWF on request.

Hersbach H., 2008, CMOD5.N: A C-band geophysical model function for equivalent wind, *ECMWF Technical Memorandum* **554**, ECMWF, Reading, UK. Available online from:
http://www.ecmwf.int/publications/library/do/references/show?id=88479

Hersbach H., Abdalla S., and Bidlot J. R., 2007b, Long Term Assessment of ERS-1 and ERS-2 Wind and Wave Products, Procedings of the ENVISAT and ERS Symposium, Montreux, Switzerland, 23-27 April 2007.

IFS documentation, (2004). edited by P. White, http://www.ecmwf.int/research/ifsdocs/CY28r1/

Isaksen, L., and Janssen P. A. E. M. (2004). The benefit of ERS Scatterometer Winds in ECMWF's variational

assimilation system. Q. J. R. Meteorol. Soc. **130** 1793-1814,

Janssen, P. A. E. M. (2004). *The interaction of ocean waves and wind.*, Cambridge Univ. Press, 300p.

Janssen, P. A. E. M., B. Hansen, and Bidlot J. R. (1997). Verification of the ECMWF wave forecasting system against buoy and altimeter data, *Wea. Forecasting*, **12,** 763-784.

Portabella M., and Stoffelen A., 2007. Development of a global Scatterometer Validation and Monitoring, to appear at: http://www.knmi.nl/publications/

Stoffelen, A. C. M., and Anderson D. L. T. (1997). Scatterometer Data Interpretation: Derivation of the Transfer Function CMOD4, *J. Geophys. Res.*, **102** (C3) 5,767-5,780.

Uppala, S. M., Kållberg, P. W., Simmons, A. J., Andrae, U., Da Costa Bechtold, V., Fiorino, M., Gibson, J. K., Haseler, J., Hernandez, A., Kelly, G. A., Li, X., Onogi, K., Saarinen, S., Sokka, N., Allan, R. P., Andersson, E., Arpe, K., Balmaseda, M. A., Beljaars, A. C. M., Van De Berg, L., Bidlot, J., Bormann, N., Caires, S., Chevallier, F., Dethof, A., Dragosavac, M., Fisher, M., Fuentes, M., Hagemann, S.; Hólm, E., Hoskins, B. J., Isaksen, L., Janssen, P. A. E. M., Jenne, R., McNally, A. P., Mahfouf, J. F., Morcrette, J. J., Rayner, N. A., Saunders, R. W., Simon, P., Sterl, A., Trenberth, K. E., Untch, A., Vasiljevic, D., Viterbo, P., Woollen, J. (2005). The ERA-40 re-analysis *Quart. J. Roy. Meteor. Soc.* **131**, 2961-3012.